Arctic Science

The Northwest Territories Thermokarst Mapping Collective: a northern-driven mapping collaborative toward understanding the effects of permafrost thaw

Steven V. Kokelj [a], Tristan Gingras-Hill[b], Seamus V. Daly[c], Peter D. Morse [d], Stephen A. Wolfe [d], Ashley C.A. Rudy[a], Jurjen van der Sluijs [e], Niels Weiss [a], H. Brendan O'Neill [d], Jennifer L. Baltzer [f], Trevor C. Lantz [g], Carolyn Gibson[h], Dieter Cazon[i], Robert H. Fraser[j], Duane G. Froese[k], Garfield Giff[l], Charles Klengenberg[m], Scott F. Lamoureux[n], William L. Quinton[o], Merritt R. Turetsky[p], Alexandre Chiasson [k], Celtie Ferguson[l], Mike Newton[g], Mike Pope[n], Jason A. Paul[f], M. Alice Wilson [a], and Joseph M. Young [k]

[a]Northwest Territories Geological Survey, Government of the Northwest Territories, Yellowknife, NT X1A 2L9, Canada; [b]Department of Biology, Wilfrid Laurier University, Yellowknife Office, Waterloo, ON N2L 3C5, Canada; [c]Department of Geography and Environmental Studies, Wilfrid Laurier University, Yellowknife Office, Waterloo, ON N2L 3C5, Canada; [d]Geological Survey of Canada, Natural Resources Canada, Ottawa, ON K1A 0E8, Canada; [e]Northwest Territories Centre for Geomatics, Government of the Northwest Territories, Yellowknife, NT X1A 2L9, Canada; [f]Biology Department, Wilfrid Laurier University, Waterloo, ON N2L 3C5, Canada; [g]School of Environmental Studies, University of Victoria, Victoria, BC V8W 3P2, Canada; [h]Integrative Biology, University of Guelph Guelph, ON N1G 2W1, Canada; [i]Łı́ı́dlı̨ Kų́ę́ First Nation, Lands & Resources, Fort Simpson, NT X0E 0N0, Canada; [j]Canada Centre for Mapping and Earth Observation, Natural Resources Canada, Ottawa, ON K1A 0G1, Canada; [k]Department of Earth and Atmospheric Sciences, University of Alberta, Edmonton, AB T6G 2E3, Canada; [l]Aurora Research Institute, Inuvik, NT X0E 0T0, Canada; [m]Inuvialuit Land Administration, Inuvialuit Regional Corporation, Inuvik, NT X0E 0T0, Canada; [n]Department of Geography and Planning, Queen's University, Kingston, ON K7L 3N6, Canada; [o]Department of Geography and Environmental Studies, Wilfrid Laurier University, Waterloo, ON N2L 3C5, Canada; [p]Institute of Arctic and Alpine Research, University of Colorado Boulder, Boulder, 80309 CO, USA

Corresponding author: **Steven V. Kokelj** (email: steve_kokelj@gov.nt.ca)

Abstract

This paper documents the first comprehensive inventory of thermokarst and thaw-sensitive terrain indicators for a 2 million km^2 region of northwestern Canada. This is accomplished through the Thermokarst Mapping Collective (TMC), a research collaborative to systematically inventory indicators of permafrost thaw sensitivity by mapping and aerial assessments across the Northwest Territories (NT), Canada. The increase in NT-based permafrost capacity has fostered science leadership and collaboration with government, academic, and community researchers to enable project implementation. Ongoing communications and outreach have informed study design and strengthened Indigenous and stakeholder relationships. Documentation of theme-based methods supported mapper training, and flexible data infrastructure facilitated progress by Canada-wide researchers throughout the COVID-19 pandemic. The TMC inventory of thermokarst and thaw-sensitive landforms agree well with fine-scale empirical mapping (69%–84% accuracy) and aerial inventory (74%–96% accuracy) datasets. National- and circumpolar-scale modelling of sensitive permafrost terrain contrasts significantly with TMC outputs, highlighting their limitations and the value of empirically based mapping approaches. We demonstrate that the multiparameter TMC outputs support a holistic understanding and refined depictions of permafrost terrain sensitivity, provide novel opportunities for regional syntheses, and inform future modelling approaches, which are urgently required to comprehend better what permafrost thaw means for Canada's North.

Key words: permafrost, thermokarst, periglacial, terrain sensitivity, climate change

1. Introduction

1.1. Background

Circumpolar landscapes are among the most sensitive environments in the world due to the rapid rates of warming compounded by the effects of permafrost thaw. Climate change and natural and anthropogenic disturbances can degrade ice-rich permafrost (Smith et al. 2010; Kokelj et al. 2017; Biskaborn et al. 2019), altering the frozen foundation of northern terrain and leading to the formation of thermokarst landforms (Fig. 1) (Kokelj and Jorgenson 2013). The initiation or acceleration of thermokarst processes, mainly involving thaw subsidence, can rapidly

Fig. 1. Thermokarst and periglacial landform diversity in northwestern Canada. (A) Thawing slopes and mass wasting showing (Ai) a deep seated, bedrock-controlled rotational failure, Mackenzie Foothills; (Aii) active-layer detachment slides in gullied terrain at Reindeer Station, Caribou Hills; and (Aiii) retrogressive thaw slumps (RTS) in fluvially incised, ice-rich glaciated permafrost terrain, Richardson Plateau. (B) Thermokarst and periglacial features in terrain with thick organic soils showing (Bi) a thermokarst affected peatland underlain by thin, ice-rich permafrost in the Bulmer Plain characterized by collapsed scar wetlands and basin-shaped wetlands connected by dendritic drainage; (Bii) a polygonal peatland with rectangular drainage in the foreground with the transition to patterned fen (string bog) with collapse scar wetlands and multibasinal drainage in the background, Great Slave Uplands; and (Biii) ice-wedge trough ponding in a polygonal peatland with rectangular drainage, Tuktoyaktuk Coastlands. (C) Thermokarst lake examples showing (Ci) ramparted lake–lithalsa (RL–L) complex in ice-rich, poorly drained glaciolacustrine deposits in discontinuous permafrost of the Great Slave Lowland; (Cii) a drained lake basin with residual ponds in the Tukoyaktuk Coastlands; and (Ciii) a thaw-slump affected tundra lake in ice-rich moraine, Caribou Hills. Photographs credited to the Northwest Territories Geological Survey (NTGS).
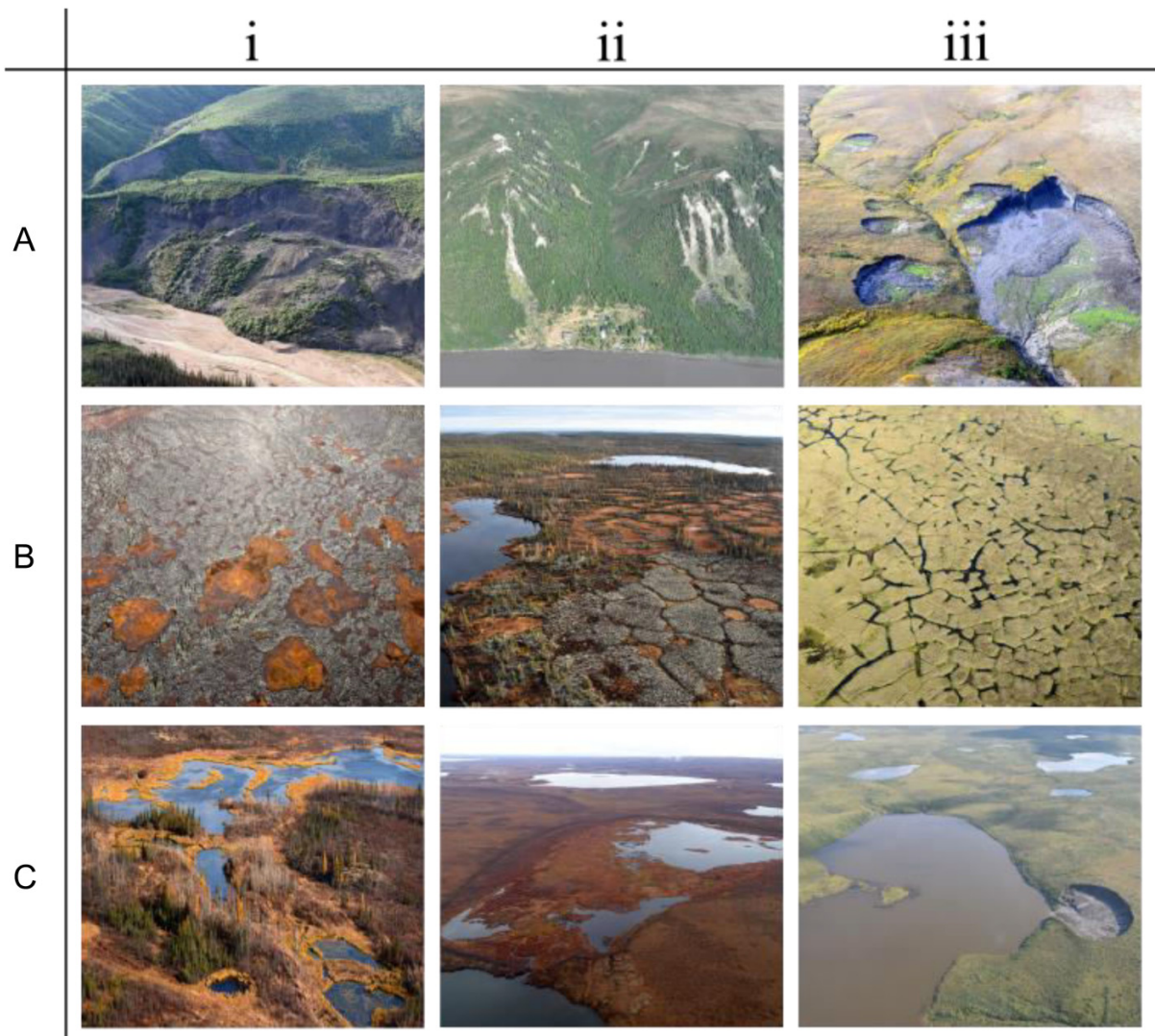
modify landscape morphology (van der Sluijs et al. 2018), hydrology (Connon et al. 2018), biogeochemical regimes (Tank et al. 2020), climate feedbacks (Turetsky et al. 2020), and the structure and functioning of northern ecosystems (Lantz et al. 2009; Chin et al. 2016; Schuur and Mack 2018). Thermokarst accelerated by a warmer and wetter climate has emerged as a stressor to the integrity of northern infrastructure (Bush and Lemmen 2019; GRID-Arendal 2020) and traditional land use and food security of Indigenous communities (Calmels et al. 2015; Spring et al. 2018). The nature and magnitude of thaw-driven landscape change are closely related to specific terrain, ground ice, soil, ecological, and climate conditions, producing a diversity of thermokarst and periglacial landforms (Fig. 1) that are valuable indicators of terrain sensitivity (Jorgenson et al. 2015). This suite of permafrost processes can lead to the formation of discrete features, such as retrogressive thaw slumps (Kokelj et al. 2015), deep-seated translational failures (Young et al. 2022), or drained lakes

(Marsh et al. 2009), or they can affect large contiguous areas where conditions give rise to distinct landscape types, such as degrading permafrost peat plateaus (Vitt et al. 1994; Quinton et al. 2011), thaw–lake complexes (Morse et al. 2017), or ice-wedge thaw ponds and polygonal-patterned ponding (Fraser et al. 2018). The terrain, environmental, carbon, and societal consequences of permafrost thaw vary with the diversity in permafrost landscapes. However, broad-scale empirical data that describe the patterns in thaw-sensitive permafrost terrain do not exist for most circumpolar regions. This significant knowledge gap constrains our understanding of the environmental effects of permafrost degradation, and the evaluation of remote sensing and spatial modelling products that predict the consequences of thaw-driven change, limiting our ability to inform climate change planning and adaptation.

An increasing amount of circumpolar-scale remote sensing and modelling products are highlighting the global significance of thermokarst and permafrost thaw (Olefeldt et al. 2016; Chadburn et al. 2017; Hjort et al. 2018; Karjalainen et al. 2020). However, fine-scale information generated through a range of methods commonly focused on development corridors or communities (Wolfe et al. 2014; Sladen et al. 2022; Allard et al. 2023) is required to support environmental and infrastructure management and climate change adaptation planning. Optical, thermal, radar, or laser scanning methods are used to map permafrost terrain conditions across fine (10^1–10^3 km^2) and intermediate (10^3–10^4 km^2) spatial scales, and they often focus on specific thermokarst processes or thaw-sensitive landforms (Aylsworth et al. 2000; Quinton et al. 2011; Segal et al. 2016; Steedman et al. 2017; Wolfe and Morse 2017; Fraser et al. 2018; van der Sluijs et al. 2018; Zwieback et al. 2018; Lewkowicz and Way 2019; Turner et al. 2021; Wang et al. 2023). These datasets are usually geographically limited by the logistical and operational constraints associated with detailed mapping. In contrast, rule-based schemes have been implemented in GIS platforms to estimate broad-scale distributions of thaw-sensitive landscapes or ice-rich terrain. These studies can use expert knowledge in a collaborative framework to approximate the distribution of thermokarst terrain and associated carbon storage (Olefeldt et al. 2016) or portray spatial patterns of thaw-sensitive or ice-rich terrain by integrating an existing knowledge base (O'Neill et al. 2019). These modelling approaches generate spatial data rapidly and have had high uptake among users due to their broad geographical coverage. They are also used as inputs for modelling climate change effects, such as global-scale estimates of carbon release (Turetsky et al. 2020) or thaw-driven impacts on water resources (Spence et al. 2020). However, rule-based GIS modelling schemes are inherently constrained by the existing state of scientific knowledge, the variable quality and resolution of input data layers, and the paucity of robust validation datasets. Consequently, they are of limited utility where fine-scale information or quantitative representation of terrain conditions are required (Gibson et al. 2021; Allard et al. 2023).

The need for acquiring fine-scale information on terrain and permafrost conditions across broad spatial scales is being partially overcome by rapid advances in Earth observation sensors, data acquisition platforms, and processing power (Chen and Wang 2018; Giuliani et al. 2019), which have accelerated remote detection of thaw-driven permafrost landscape change at multiple spatial scales (Fraser et al. 2018; Nitze et al. 2018). Machine learning techniques hold significant promise for automating image analyses to recognize fine-scale spatial patterns of Earth surface processes and landforms, with applications to the vast, rapidly changing, and remote permafrost environments (Siewert 2018; Huang et al. 2020). Machine learning requires systematically collected fine-scale training data from a variety of locations, but robust training and validation datasets of permafrost and periglacial processes remain sparse. The automation of Earth observation and rapid progress in modelling permafrost change at broad spatial scales heightens the need for complementary efforts in advancing empirical mapping of thermokarst terrain for training and validation and to foster a field-based understanding of the thaw-driven processes that are transforming permafrost environments.

1.2. The Northwest Territories Thermokarst Mapping Collective

Climate change has major environmental and societal implications for northwestern Canada's rapidly warming and ice-rich permafrost regions (Kokelj et al. 2021; Smith et al. 2022). The Northwest Territories (NT) covers an area of 1.346 million km^2 and comprises much of Canada's most ice-rich permafrost terrain (Fig. 2) (O'Neill et al. 2019). The study region is also comprised of diverse ecoregions that host a significant portion of northern Canada's community, transportation, mining, and oil and gas infrastructure. The NT comprises the traditional territories of several Indigenous groups who are reclaiming decision-making authority through the establishment of seven regional and three community-based governments that have been negotiated, or are in the process of negotiating self-government agreements with the Government of the NT (GNWT) and the Government of Canada (https://www.eia.gov.nt.ca/en/indigenous-governments). Northern regulators, planners, policy-makers, and communities require better information to understand the environmental and societal implications of permafrost thaw and expressly recognize the need for improved permafrost mapping to support decision-making (GNWT 2018). The Arctic science community has mobilized to examine the physical, chemical, biological, and carbon consequences of permafrost thaw and has attempted to upscale results to broad regional and circumpolar scales (Spence et al. 2020; Turetsky et al. 2020), but many potential analyses require information on the spatial distribution and configuration of thaw-sensitive permafrost terrain. Despite these growing societal and scientific needs, no systematic, empirical inventories of thaw-sensitive permafrost terrain exist for most of the circumpolar world.

To address this significant knowledge gap, the NT Geological Survey (NTGS) initiated the NT Thermokarst Mapping Collective (TMC) in collaboration with Wilfrid Laurier University (WLU), the Geological Survey of Canada (GSC), and other government, academic, and Indigenous partners. The overarch-

Fig. 2. Study area map showing the project boundary defined as the Northwest Territories (NT) border to the southern limit of discontinuous permafrost plus a 100 km southward buffer, the continuous permafrost zone in transboundary watersheds, northward drainage areas into the Beaufort Sea, and $75 \times 75\,\mathrm{km}^2$ areas around all NT communities. The $2\,023\,972\,\mathrm{km}^2$ study area is divided into 32 128 grid cells that are $7.5 \times 7.5\,\mathrm{km}^2$. The map highlights focal areas where preliminary results have been compiled and are presented in this paper. Some study area boundaries follow watershed divides from the National Hydro Network geodatabase (Natural Resources Canada 2016). The permafrost boundaries are from Brown et al. (2002). Level IV ecoregions are from Ecosystem Classification Group (2008, 2012).
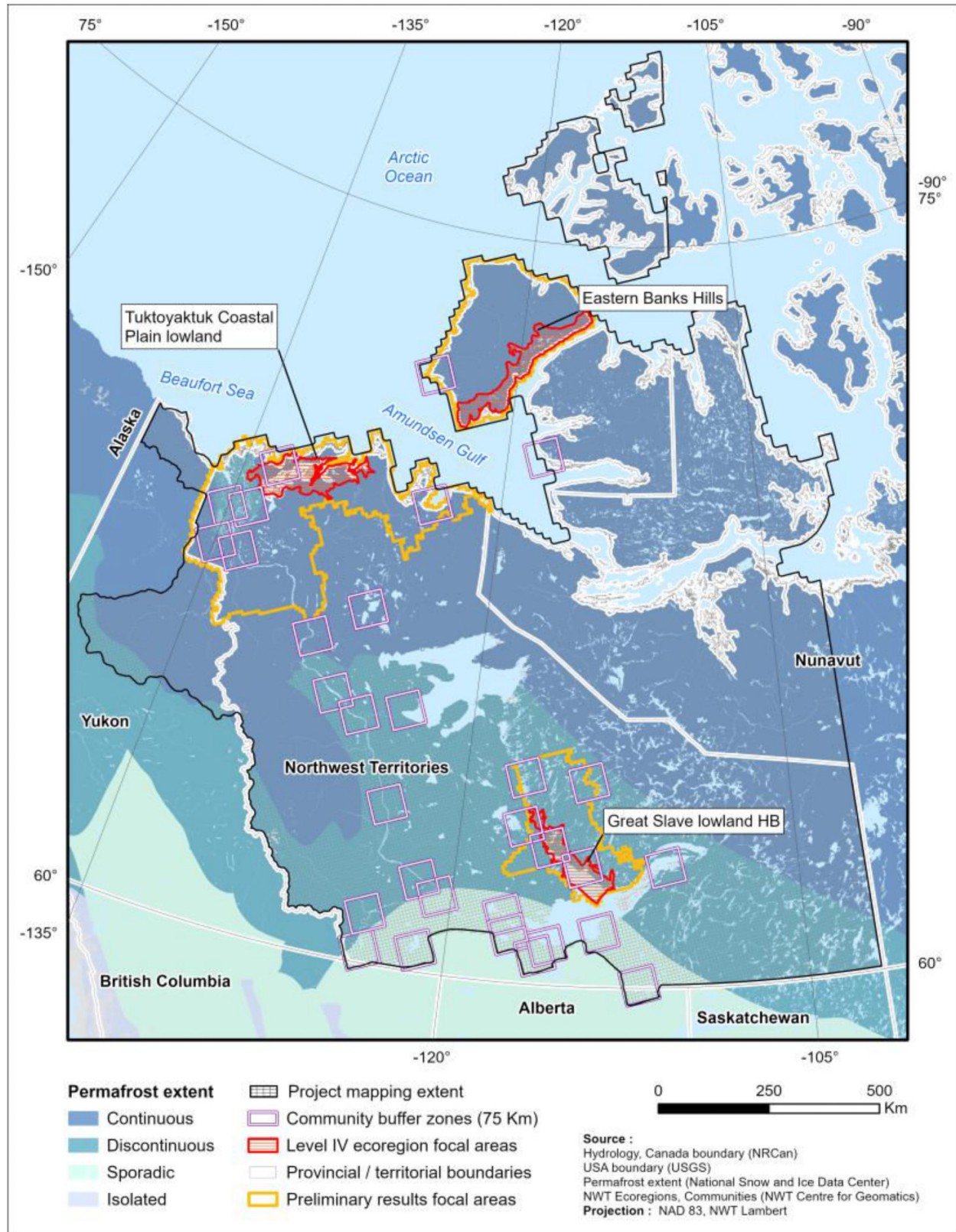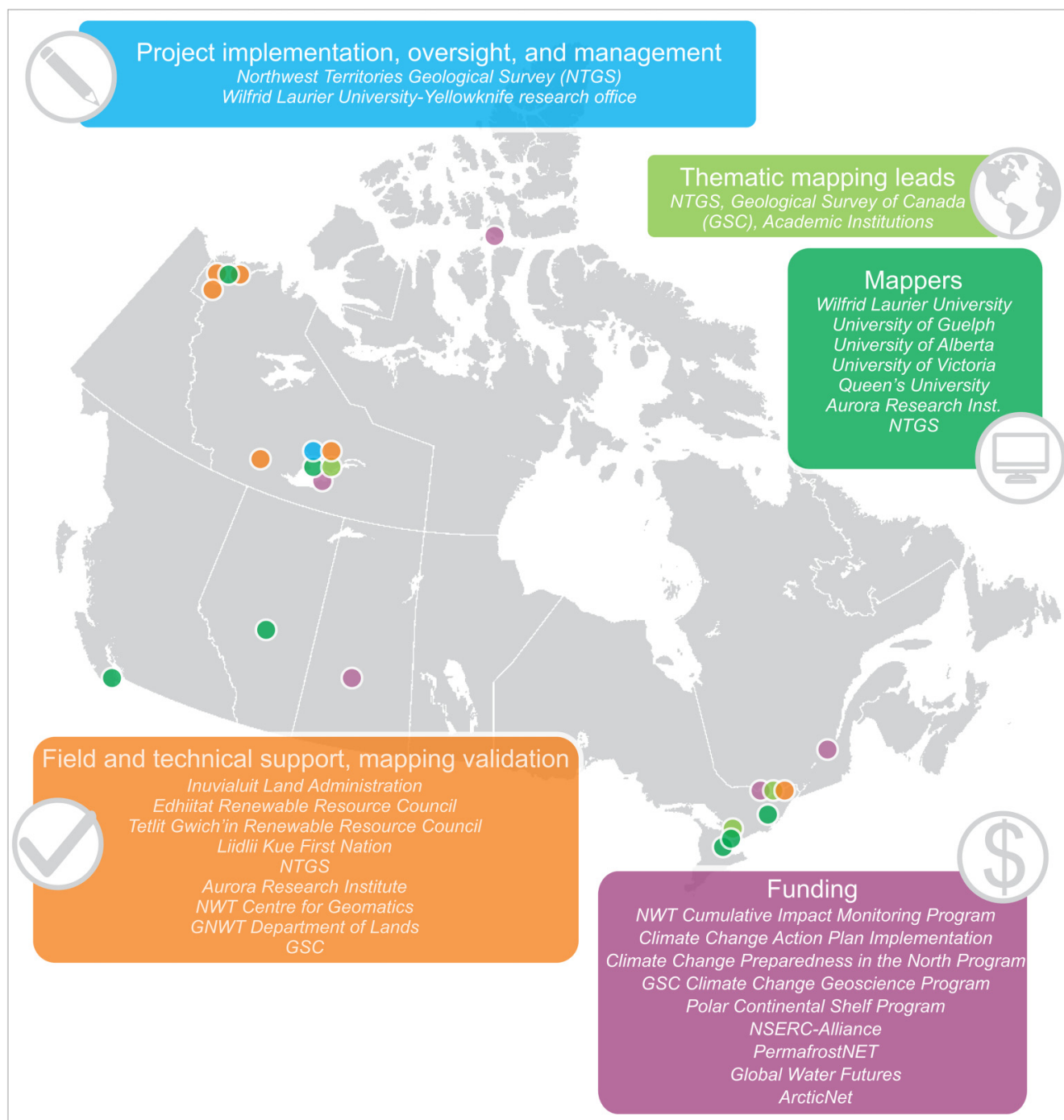
Fig. 3. Project organization, roles and institutional involvement by location.

ing aim of the TMC is to advance knowledge of permafrost terrain conditions and thermokarst distribution across NT and its permafrost-affected transboundary watershed areas (Fig. 2), within a framework where partners co-develop scientific knowledge and its dissemination. While this has become best practise in northern ecology (Johnson et al. 2015; Cold et al. 2020; Thompson et al. 2020; Chila et al. 2022), the general approach is still emerging in the field of permafrost science. To focus the project and address northerners' needs, the TMC fostered collaborations across disciplines and among organizations to develop a systematic approach to map and inven-

tory thermokarst terrain under the groupings of slopes and mass wasting, periglacial, and hydrological themes, establish a spatial data infrastructure (SDI) and management framework, and train mappers from across Canada (Fig. 3). Following methods developed by the TMC, and using ArcMap 10.8., and now ArcGIS Pro, the mappers populated a gridded vector geodatabase of the study area by (1) systematically inspecting true colour and near-infrared Sentinel-2 satellite imagery at a 1:20 000 scale for the presence and relative abundance of indicators of sensitive permafrost terrain according to criteria defined by expert teams and (2) recording the observa-

tions within each 7.5 × 7.5 km² grid cell by populating its attributes in the geodatabase according to lists of descriptors for each feature or terrain type (Figs. S1 and S2) (e.g., Gibson et al. 2020; Wolfe et al. 2022). The resulting empirical data will provide detailed information on the patterns and characteristics of sensitive permafrost terrain throughout the study area (Fig. 2).

The objectives of this paper are to (1) describe the organizational framework and general methodologies developed to implement the TMC project; (2) explain the SDI to support data sharing needs; (3) explore preliminary thermokarst mapping outputs through comparisons with published fine-scale datasets (10³ km²) as a validation of the approach, and with broad-scale national and circumpolar datasets (10⁵ km²) to explore the patterns of variation and the value of the TMC data; and (4) highlight the diversity of thermokarst-affected landscapes being quantified by these methods. This project overview and preliminary results provide a basis for discussing some limitations of the approach, and the challenges and opportunities of developing a broad-based, cross-disciplinary permafrost research collaboration, the need for linking field-scale knowledge with mapping and modelling outputs, and the benefits for advancing permafrost science and its application. In addition, we address the need for more holistic, geomorphically based frameworks to advance knowledge of the thaw sensitivity of permafrost terrain. Finally, we highlight opportunities for enhancing collaboration and knowledge sharing between northerners, scientists, environmental managers, and Indigenous partners through experiences gained in this project.

2. Study area and terrain conditions

The project mapping domain was initially set as the NT boundaries. Subsequently, the margins were refined by a 100 km buffer south of the discontinuous permafrost boundary and expanded to transboundary watersheds adjacent to the NT that drain the northern margins of discontinuous and continuous permafrost regions, notably the Peel watershed, and watersheds draining into the Beaufort Sea. This includes all of Victoria Island and the northwestern wedge of mainland Nunavut adjacent to the NT, containing transboundary waters. Buffer zones (75 × 75 km²) were established around all NT communities and mapping was prioritized there in response to stakeholder needs (Fig. 2). The mapping extent was constrained by 2016–2017 peak-summer visible and false colour orthomosaics of publicly available Sentinel-2 imagery at 10 m spatial resolution, which was the foundational dataset used in this inventory. The study area consisted of 32 138 grid cells (7.5 × 7.5 km grid), covering an area of 2 023 972 km² and excludes those covered entirely by water.

The study area extends from 60° to 79°N latitude spanning diverse physiography, geology, ecology, climate, and permafrost conditions (Figs. 2 and S3) (Slaymaker and Kovanen 2017). The central Taiga Plains region is dominated by mixed and coniferous forest cover, characterized by low-lying sedimentary bedrock plains and plateaus overlain by thick unconsolidated sediments. Extensive organic deposits cover the

central Mackenzie Valley and commonly host thaw-sensitive permafrost (Aylsworth and Kettles 2000; Ecosystem Classification Group 2009). This ecozone includes the Mackenzie River watershed from the Beaufort Sea coast in the north to the southern NT border and merges with the temperate Boreal Plains in the south. The western margin of the study area hosts higher elevation, mountainous and hilly terrain of the Taiga and Boreal Cordillera, where Cordilleran and Laurentide ice sheets merged during the last glacial interval. The river valleys are topographically controlled and incise tills and glaciolacustrine deposits in their lower reaches (Ecosystem Classification Group 2010). To the east, the lower-lying Taiga Shield is underlain by igneous and metamorphic bedrock, characterized by a mosaic of exposed bedrock and a thin mantle of till, glaciofluvial, and glaciolacustrine deposits. The topography and drainage patterns of this lake-rich landscape are predominantly bedrock fault-controlled (Ecosystem Classification Group 2008). Higher latitudes of the study area include the Southern and Northern Arctic ecozones underlain by igneous and metamorphic bedrock of the Canadian Shield in the southeast and sedimentary bedrock to the north extending onto the Arctic Islands (Ecosystem Classification Group 2008). The Laurentide ice sheet covered most of the study area (Dyke and Prest 2008), resulting in a complex system of glacially derived landforms and sediments, which commonly host ice-rich permafrost (O'Neill et al. 2019). A cold continental and Arctic climate through the Holocene produced permafrost that is continuous in extent across the northern half of the study area, and discontinuous to sporadic in the south (Fig. 2).

The evolution of ground ice and terrain conditions yield distinct periglacial and thermokarst landforms. Our research interests arise from the need to identify and inventory these indicators of thaw sensitivity because much of the NT is underlain by ice-rich permafrost (O'Neill et al. 2019 and references within). Major ground ice types are relict massive ice preserved since deglaciation, with exposed deposits largely constrained to ice-marginal landscapes that are widespread across the western Arctic (Kokelj et al. 2017). Basal glacier ice has been preserved in these environments (Murton et al. 2005), though in certain cases segregated–intrusive ice developed as permafrost aggraded into sediment deposits in association with the retreating ice sheet (Rampton 1988). Segregated ground ice is most commonly associated with the post-glacial establishment of permafrost across glaciolacustrine deposits in fine-grained tills and in more recently exposed environments, such as drained lakes or emergent shorelines (O'Neill and Burn 2012; Lantz et al. 2022), where organic deposits also typically accumulate (Aylsworth and Kettles 2000). Upward aggradation of permafrost into fine-grained sediments in association with ecological succession, climate shifts, or colluvial and alluvial processes results in the development of near-surface segregated ice, which is ubiquitous in many terrain types across large areas of the study region (Mackay 1972; Kokelj and Burn 2003, 2005; Paul et al. 2021). The persistence of cold climate conditions has promoted ice-wedge development, which manifests as polygonal networks widespread in subarctic and tundra environments of northwestern Canada (Mackay 1972; Kokelj et al. 2014). General as-

sociations may be recognized between permafrost zone, terrain and climate history, ground ice, and thermokarst landform types; however, knowledge of how these landforms are distributed and combined to manifest as terrain assemblages remain poorly understood across spatial scales. Figures S1, S2, and Appendix A provide a summary and examples of the thermokarst and periglacial landforms inventoried in this study.

3. Project and mapping approach and methods

3.1. Project and mapping approach and methods

An extensive set of landforms indicative of thermokarst or permafrost sensitivity related to mass wasting, hydrological, or periglacial processes occur within the study area. These landforms are related to the suite of geological, ground ice, climate, and ecological factors that reflect variation in landscape history (e.g., Wolfe and Morse 2017; Kokelj et al. 2021). Because of the diversity of thermokarst and periglacial landforms, and the distribution of collaborators situated across Canada, a wide range of expertise was leveraged to develop the methods and tools needed to support the project. The NTGS with support from the GSC and the GNWT–WLU partnership, worked with academic and Indigenous partners to initiate the TMC project. The NTGS presented a general approach to rapidly inventory landscapes affected by different permafrost features, which was discussed at a technical workshop held in Yellowknife, NT in March 2018. Decision-makers and northern partners' needs were determined through continued discussions with stakeholders, which together established the goal of developing territory-wide mapping of thaw-sensitive landforms. The refinement of methods for producing empirically based permafrost maps was advanced following input from this workshop, as well as activities focused on the pursuit of project funding. Participants formed expert teams to develop mapping methodologies within themes of thaw-driven landforms. The NTGS provided project oversight, and the primary theme leads from the Territorial and Federal Geological Surveys, and university researchers co-developed the scientific approach (Fig. 3). The GNWT–WLU partnership enabled the staffing of a Yellowknife-based project coordinator who reported to the TMC project. This northern-based position has worked with NTGS to advance the project by coordinating participants, developing the SDI, managing data, and supporting project reporting functions. Several funding partnerships were secured with organizations across the NT and Canada to train mappers and support mapping (Fig. 3). Linkages with community partners related to this project have been initiated through workshops and field programs but were severely hampered by COVID-19 restrictions. The northern research partners' abilities to sustain field programs through the pandemic provided opportunities to work with Indigenous partners for training in permafrost observational methods and for aerial validation of the mapping during the 2020–2022 field seasons.

3.2. Mapping framework and generating a grid-based dataset

The methodology implemented by the TMC builds upon an approach described in detail by Segal et al. (2016) and employed by Kokelj et al. (2017) who used 10 m resolution SPOT 4/5 satellite imagery (from 2005 to 2010) to identify thaw-driven mass wasting features within a standardized grid of $15 \times 15 \, \text{km}^2$ cells throughout northwestern Canada. The uniquely identified grid cells are used to partition and attribute observations of terrain features into a set of discrete mapping units, which can then be used to quantitatively evaluate spatial variation. After some testing, the TMC used uniquely identified quartiles (i.e., $7.5 \times 7.5 \, \text{km}^2$) of the grid system from Segal et al. 2016, significantly improving resolution and resulting in mapping units deemed to be of sufficient granularity to produce a valuable broad-scale inventory of permafrost landscape characteristics over the entire study area in a timely manner (Fig. 4). Grid cells entirely over water, such as in the ocean or in the middle of Great Bear or Great Slave lakes, were removed from the database using the Canada Coastline and inland lake boundaries (Natural Resources Canada 2016). The TMC developed guidance documents to describe methods for inventorying mass wasting, hydrological, and periglacial features, supporting the design of a geodatabase in ArcMap 10.8 to enable mappers to identify and attribute the landforms or terrain features that characterize each grid cell. Procedural manuals for inventorying hydrological features and peatlands, including intermapper comparisons for permafrost peatland identification are published as NTGS Open Reports (e.g., Gibson et al. 2020; Wolfe et al. 2022). The procedural manual for inventorying mass wasting features builds on Segal et al. (2016) and along with the manual for periglacial features are in the process of publication as NTGS Open reports. The raster datasets from which the inventory data were derived, and the supporting data layers, are summarized in Table S1. Thematic or regionally focused spatial datasets will accompany scientific publications.

3.3. Rubric development and mapping

The purpose of the grid-based approach is to build an initial inventory of feature presence and relative abundance over large areas (Segal et al. 2016; Ramsdale et al. 2017; Chiasson and Allard 2022). Here, we summarize how the rubrics to identify and interpret thermokarst and periglacial features on the satellite imagery were developed, and how inventory data were recorded and integrated into an SDI, and we touch on some limitations of the mapping approach. More detailed explanations of the methods and feature interpretation criteria upon which the mapping was based are provided in NTGS Open Reports that were developed (Gibson et al. 2020; Wolfe et al. 2022) or are being refined and published with anticipated, theme-specific research papers. For the retrogressive thaw slump (RTS), polygonal terrain, and ramparted lake–lithalsa (RL–L) terrain maps presented in this paper, Appendix A provides several examples of each of these landforms in an oblique aerial image and its appearance on SPOT 6/7 imagery (2018) and Sentinel-2 imagery (2016–2017). The general approach and geodatabase structure ensured that the data types

Fig. 4. Mapping area and grid-based mapping structure for the TMC. (A) The grid cells focus on the Northwest Territories (NT) and associated transboundary watersheds and exclude those that are entirely consisted of water. Mapping rubrics were tested and first advanced within 75×75 km^2 windows centered on each of the 33 NT communities as indicated by dark grey squares. (B) The core element of mapping is a 15×15 km^2 grid cell that is divided into four quartiles. Each quartile possesses a unique identifier to facilitate data tracking and analysis. The community test windows are composed of 25 core grid cells and 100 quartiles. (C) Sentinel-2 imagery associated with quartile FF 180.2 and part of the mass wasting data table showing retrogressive thaw slumps, mega slumps, shallow landslides, and gullied terrain on the fluvially incised Peel Plateau, northwestern NT. Some study area boundaries follow watershed divides from the National Hydro Network geodatabase (Natural Resources Canada 2016). The imagery in (C) is peak-summer false colour orthomosaiced Sentinel-2 imagery (European Space Agency, Copernicus Sentinel data). The map projection is NAD 83, NWT Lambert.
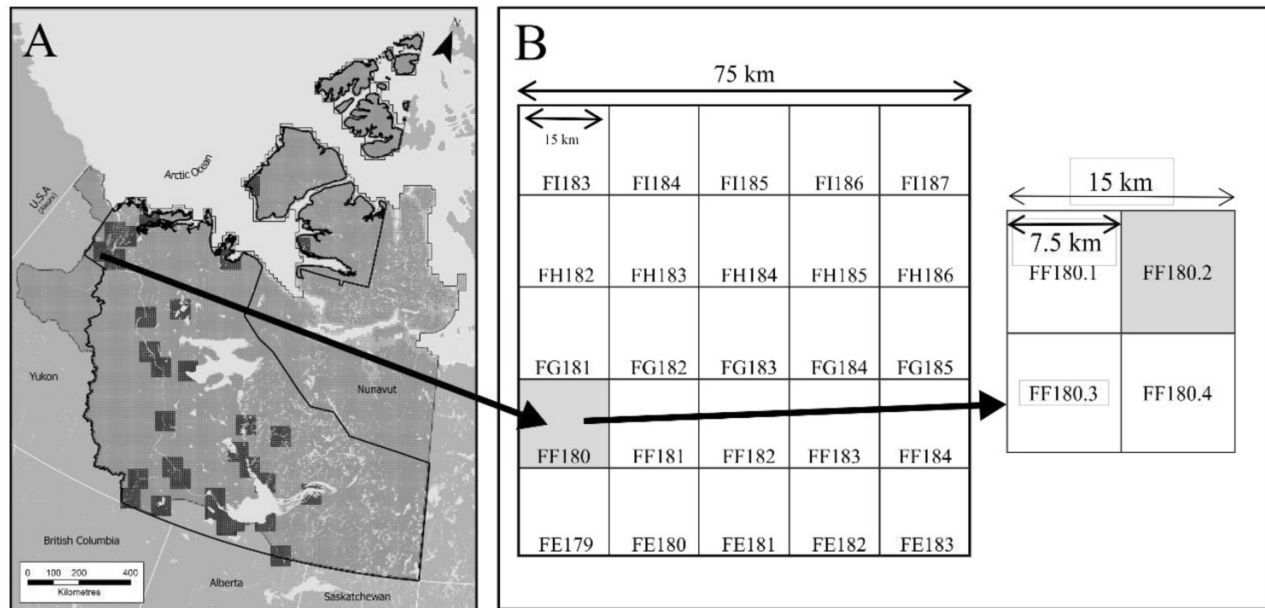

are correct, data entry is logical and consistent, and database entries are unique.

Permafrost experts initially advanced the mapping workflow by creating a comprehensive list of thermokarst landforms and indicators of permafrost thaw sensitivity and their morphological attributes (Fig. 5). Features were categorized into themes according to geomorphic processes and environmental setting: (1) mass wasting (e.g., Segal et al. 2016), (2) hydrological features (Wolfe et al. 2022), and (3) periglacial features. An organic theme (Gibson et al. 2020) focused on identifying the presence and abundance of peat plateaus as indicators of thaw-sensitive permafrost and at a higher spatial resolution, so it was merged with the periglacial theme where attributes describing peatland morphology and the nature of degradation patterns had been developed. The list of features and attributes included in each theme was refined as leads

Fig. 5. Architecture of the Northwest Territories (NT) Thermokarst Mapping Collective (TMC). Rubric development included refining the list of landforms that could be identified on Sentinel-2 imagery (2016–2017; 10 m resolution). Descriptive attributes were added to maximize inventory information for each 7.5 × 7.5 km² grid cell. Mappers from several partnering institutions were then provided with the database to inventory designated areas.
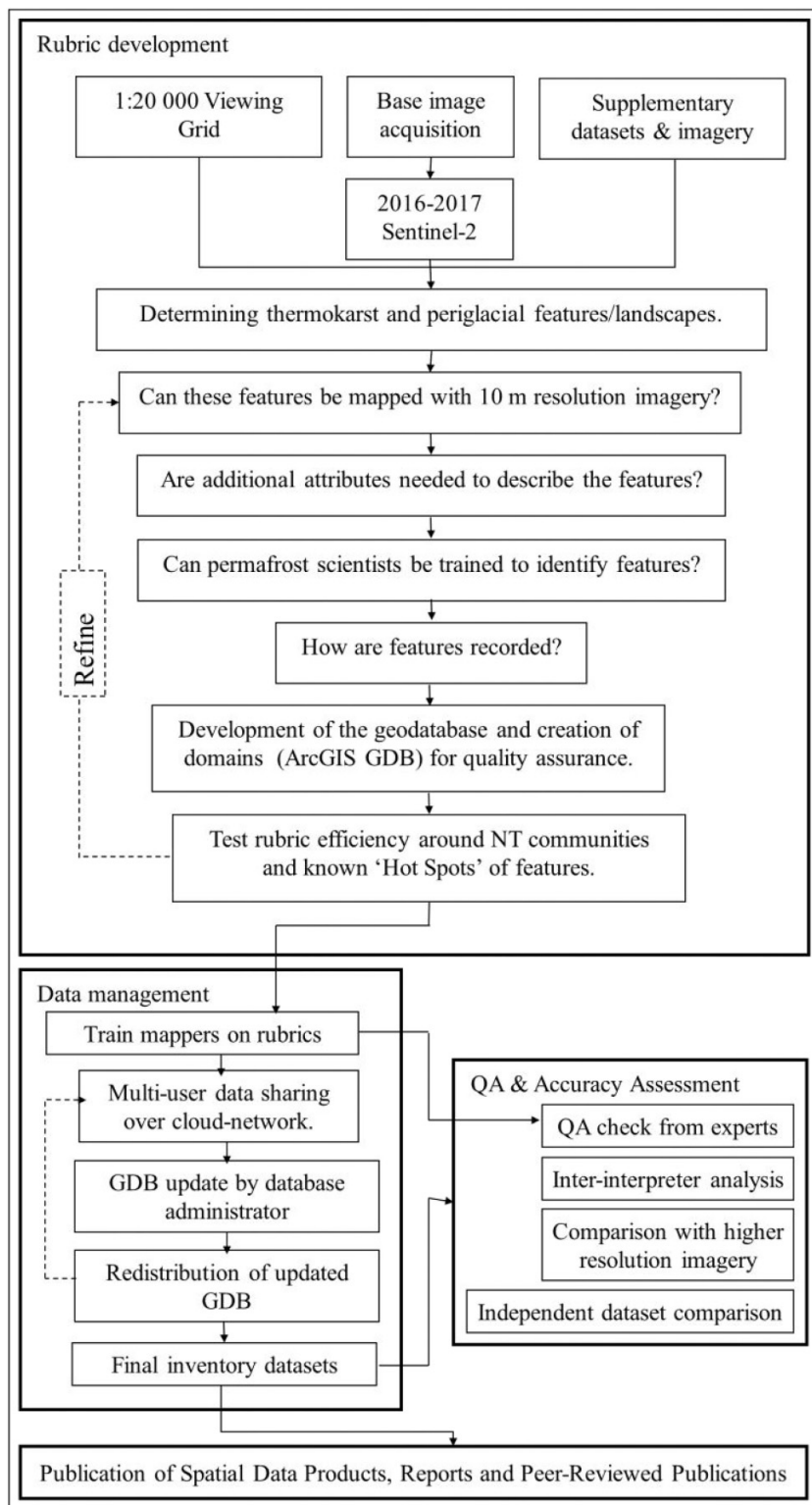
and mappers learned by locating, identifying, and attributing landforms across well-studied environments using the Sentinel-2 satellite optical imagery (e.g., Appendix A). Follow-

ing Tobler's (1987) rule for depicting land use and land cover change using satellite imagery, an optimal viewing scale for the Sentinel-2 imagery was set at 1:20 000. Consequently, the

10 m resolution of Sentinel-2 imagery imposes limitations that necessitated experts to group thermokarst landforms or landscape indicators of permafrost thaw sensitivity and simplify rules for identification and attribution (Fig. S2 and Appendix A). For example, landslides were grouped generally as either "thaw slumps" or "deep", or "shallow" slides based on morphology and were not further differentiated by type. Polygonal (ice-wedge network) terrain was attributed as upland or lowland, but high- or low-centred polygons were not differentiated. Given the mapping constraints, methods were developed to identify and inventory 25 distinct thermokarst landforms or landscape indicators of permafrost thaw sensitivity according to the three primary themes, which are organized according to the spatial data model implemented in the geodatabase with corresponding primary tables (Figs. S1 and S2).

The TMC theme leads and mappers reached consensus on how to estimate counts or % cover of each feature according to bins of counts (e.g., 0; 1; >1; and >10) or approximate % cover during preliminary trials (e.g., 0; <10%; 10%–33%; 33%–66%; 66%–100%) (Figs. 4 and 5, and Fig. S2). These bins and the final set of landforms and indicators of thaw-sensitive permafrost terrain, and their attributes were informed by results of preliminary trials and mapper feedback, which followed regular online sessions with theme experts and mappers held to discuss landscape interpretations, refine rubrics, and promote iterative learning. The bins can be reduced to three categories (i.e., [absent (0); few (1); and many (2)] or [absent (0); trace cover (<10% cover); and abundant cover (>10% cover)] or further reduced to binary presence or absence, giving several categorical data formats for quantitative comparisons among landforms or with other datasets. With the feature sets, their attributes, and bins of count and cover defined, we linked the geodatabase to a GIS where mappers inspected imagery and populated the specified grid cell attributes according to theme-specific dropdown menus that reference look-up tables specifying the features and attributes (Fig. 4). The look-up tables ensured the format of the information entered is consistent and replicated by all mappers.

In order to produce a preliminary dataset for analysis and support northern needs, we prioritized 75 × 75 km² areas surrounding each of the 33 communities in NT (Figs. 2 and 4). We supported this initial landform interpretation and mapper training with knowledge from thematic experts and higher-resolution imagery (SPOT 6/7 1.5 m). To test the validity of the mappers' data, the experts performed QC checks on all data as mappers were being trained that focused discussions on refining interpretation of features. Thereafter, the experts performed QC checks at intervals guided by mapping progression. In quartiles where the lead researcher determined that the mapper incorrectly identified or attributed a landform, the researcher would manually change the recording and add their initials to a "QAQC" field in the dataset. Administrator updates to the master database involved replacing quartiles with an edited QAQC field. Custom python tools (Arcpy module) were developed and implemented to ensure that the logic model of the SDI was respected before uploading data to the master database. For example, the scripts used relationships established in the logic model (Fig. S2) to flag fields that were incorrectly left blank. These grid cells would then be checked manually by the mapper or coordinator and filled in appropriately.

The mapping approach we have implemented is inherently challenged by human error during feature identification, and by interpreter variation (Pasher et al. 2013; Brardinoni et al. 2019). Clear guidance documents that included landform examples and how they manifest on Sentinel-2 imagery was provided to mappers (Fig. S1 and Appendix A) (e.g., Wolfe et al. 2022). The TMC employed conservative identification protocols to limit false positives (commission errors). For example, only active landslides features were counted by mappers. Moreover, active retrogressive thaw slumps are typically associated with areas of past disturbance (van der Sluijs et al. 2022), so excluding stable landslides was assumed to have little effect on final results depicting broad-scale spatial patterns. We identify that cloud cover or shadow in some instances could affect feature identification but this was minimized by obtaining images with less than 10% cloud cover. If cloud cover, snow, or other factors decreased the mappers ability to confidently assess terrain conditions of a grid cell, this was indicated in the comments box. We note that the 75 × 75 km² areas around the 33 communities, spanning the diversity of terrain across the study area underwent a QC check by a second independent mapper, but a QC check will not be possible for the entire study domain consisted of over 30 000 grid cells. Interpreter variation assessments comparing permafrost peatland coverage estimates in Gibson et al. (2020) reported that overall agreement was 84% better than chance, and comparisons will be reported for other landforms with the publication of theme-specific datasets.

Upon completion of the initial testing, clarifying landform interpretations, correcting interpreter biases, and with mappers trained, the inventory effort expanded and was divided according to the NT Ecosystem Classification Group Level IV ecoregion framework. In total, NT contains 162 Level IV ecoregions characterized by distinct regional ecological factors, including climate, physiography, vegetation, soil, water, and fauna (Ecosystem Classification Group 2008, 2009, 2010, 2012, 2013). Mappers were assigned a suite of Level IV ecoregions based on their expertise, and research interests and mapping is ongoing, with 76% of the mass wasting, 40% of the periglacial, and 37% of the hydrological theme mapping completed for NT at the time of paper submission.

3.4. SDI and data management

A flexible and robust SDI was needed to accommodate the development of a data model, support the collaboration of a decentralized user base, and manage the generation of empirical permafrost data that covered a broad spatial domain. SDIs are geospatial data portals (Fig. 6A) that allow users to access remote or internal servers to connect to databases and interact with spatial data through a desktop GIS or web mapping service (Wang 2010; Maquil et al. 2018). Enterprise GIS systems allow multiple users to edit databases simultaneously (Maguire and Longley 2005; Kong 2015), common to

Fig. 6. Spatial data infrastructure (SDI) models that support the integration of data from multiple mappers: (A) Client–server architecture typically implemented in multi-user enterprise GIS systems. In the client tier, multiple mappers work on "child replicas" of the parent database hosted on the server. Server software and business rules are used to detect updated landforms; if no constraints are noticed, the updates are automatically synchronized to the parent database. (B) The TMC has used a file-based architecture to support the integration of map data from multiple interpreters, where each mapper works on a personal copy of the database and sends updates to the database administrator, who runs custom-built python scripts to ensure that data were correctly entered and merges the updates with the master database hosted on a file-sharing network.
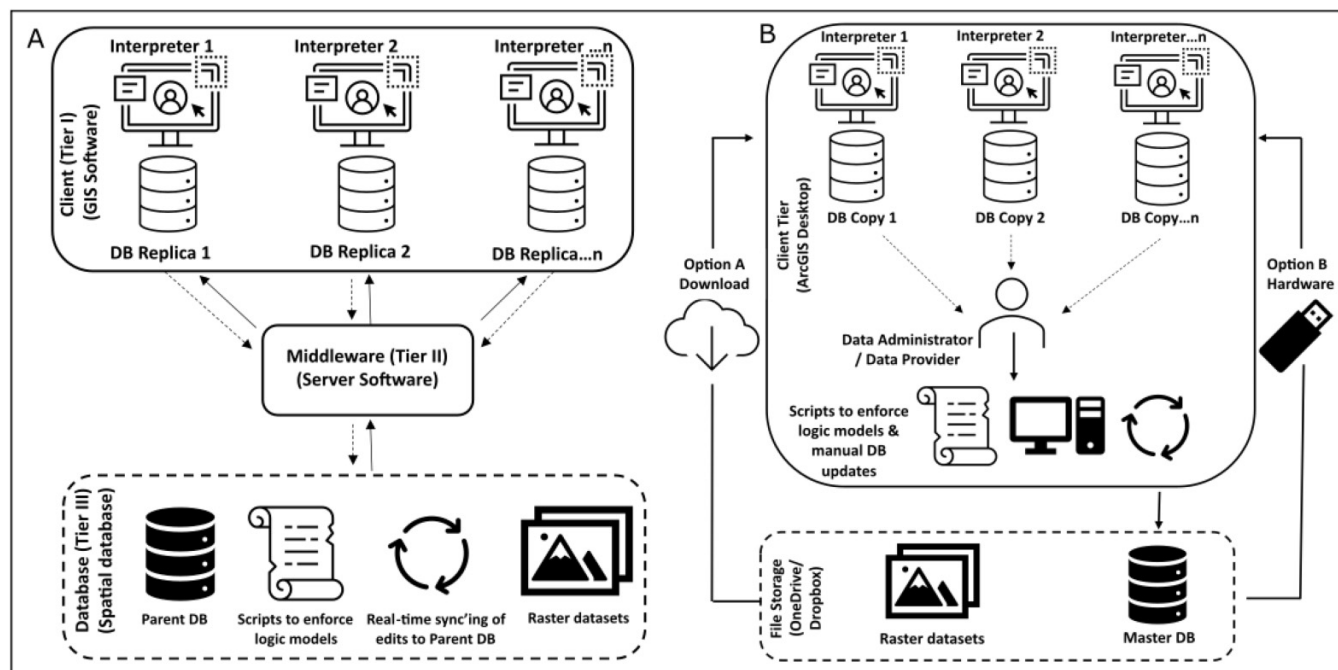
large institutions with a centralized or internal user base and dedicated resources to manage networks (Fig. 6A) (Keating et al. 2003; Esri 2022). The broad-based collaborative nature of the TMC and its modest resources required that the project coordinator with geomatics expertise developed and maintained a low-cost and easy-to-implement SDI while enabling multiple novice GIS users to edit data (Fig. 6B). The project SDI that emerged allowed mappers to view, update, edit, and attribute project data easily, and accommodated the addition of new mappers from different institutions while maintaining mapping progress.

The project applied a file-based geodatabase architecture used in desktop-based GIS that was adapted to a multi-user environment (Fig. 6B). Each TMC mapper obtained the required vector and raster datasets through file-sharing networks (i.e., cloud storage) or with physical hardware (i.e., external drives), and incrementally updated personal copies of the database. In this method, the project coordinator received the updated data and ran custom-built python scripts to perform data quality assessments. The coordinator then merged the updates with a master database through additional rule-based scripts to overcome issues with conflicted copies that can otherwise lead to loss of data and confusion (MacEachren 2001; Yovcheva et al. 2013; García-Chapeton et al. 2018). The synchronous–decentralized collaborative framework consists of users across Canada with access to the tools and training to generate systematic inventory data on thermokarst and periglacial features.

3.5. Comparisons with independent and modelled data products

Concurrent with the generation of TMC data, we also conducted NT-wide aerial inventories of thermokarst and periglacial landforms to document the nature of permafrost landscapes and support the validation of TMC outputs. A brief summary of the aerial survey approach is provided here. In the summers of 2020–2022, during the COVID-19 pandemic, northern project partners were supported by the Polar Continental Shelf Project to perform aerial inventories of thermokarst and periglacial landform features for over 37 000 km of flight lines across all major ecological regions of the NT. The team made over 7500 feature observations, recorded landform types and attributes, and obtained georeferenced images of each feature type inventoried. During 2020 fieldwork, the team iteratively refined the TMC database model (Fig. S2) to improve its suitability for aerial observations and implementation through a web-based GIS application that enables offline data collection (ArcGIS Survey123, ESRI™). The application allows users to collect GPS-attributed spatial data points on a field-based tablet (Apple iPad Mini with built-in GPS unit), and then upload observations to a cloud network (ArcGIS Online) when an internet connection is re-established. The aerial survey team comprises an expert observer who identifies and assigns attributes to a feature of interest, a photographer with a GPS-enabled DSLR camera who obtains georeferenced images of the feature, and a tech-

nician who enters the observation point, feature type, and its attributes into the Survey123 survey form. Survey rule sets and option pick lists enabled efficient data entry while ensuring that the data model was respected. The repetitive nature of this data collection provides training in thermokarst and periglacial landform identification and group learning, fostering a growing community of permafrost expertise. The aerial surveys also provided the first systematic, broad-scale, georeferenced inventory of thermokarst and periglacial features and their characteristics across NT and a unique dataset to confirm the nature and presence of landforms mapped by the TMC. We extracted the data for three feature types (RTS, polygonal terrain, and RL–L complexes) for comparisons with TMC data in the western Arctic and North Slave focal regions (Fig. 2 and Appendix A).

We also compared published, fine-scale empirical data products with these TMC datasets using confusion matrices and summarized prediction results. Here, we used high-resolution, regionally specific datasets on RTS (Lewkowicz and Way 2019), polygonal terrain (Lantz et al. 2017), and RL–L complexes (Morse and Rudy 2022) to evaluate the TMC approach and outputs. The TMC spatial outputs reflect the rapid assessment of features or landforms indicative of thermokarst or sensitive permafrost terrain that were quantified according to bins of counts or % area within each $7.5 \times 7.5 \, km^2$ quartile, whereas the independent fine-scale spatial datasets were typically polygons for spatially extensive landforms (e.g., ice-wedge polygon networks), or points for discrete features (e.g., RTS) (Appendix A). To enable comparison with the TMC grid-based inventories the validation datasets were converted to the raster framework and normalized to the TMC grid-based schema (Table S2) using a suite of geoprocessing tools.

To demonstrate the new insights that TMC datasets provide on the thaw sensitivity of permafrost terrain at broader spatial scales (10^4–$10^5 \, km^2$), comparisons were also made with national or circumpolar scale products depicting thermokarst landscapes (Olefeldt et al. 2016), sensitive ice-wedge terrain (Karjalainen et al. 2020), or ground ice abundances (O'Neill et al. 2022). To conduct the comparisons, broadscale products were also normalized to the $7.5 \times 7.5 \, km^2$ grid cells, and we retained as many of their categorical attributes as possible (Table S3). Recognizing that the nature of empirically based TMC outputs differs from the modelled permafrost characteristics or terrain susceptibility, we emphasize that these comparisons aim to highlight the value of observational datasets for better understanding the spatial variation of the indicators that characterize thaw-sensitive permafrost terrain.

4. Preliminary mapping results

4.1. Comparison with fine- and broad-scale independent datasets

Spatial patterns of active or recent retrogressive thaw slumps (RTS) on Banks Island mapped by TMC highlight the thaw sensitivity of permafrost-preserved ice-cored moraine (Fig. 7A) (Kokelj et al. 2017). A point dataset of RTS derived from the Landsat time series (Lewkowicz and Way 2019) was converted to the raster framework, and the comparison with the TMC dataset shows good (84%) agreement (Figs. 7A–7C and Table 1A). There is high correspondence in unaffected terrain (95%), but lower agreement among the various disturbance classes likely reflecting differences in imagery and methodologies used for feature counts (Table 1B). The larger bottom plate of Fig. 7D shows RTS-affected terrain mapped by TMC for a 215 426 km^2 western Arctic region of NT, which follows general patterns described in coarser resolution published products (Kokelj et al. 2017, 2021). RTS-affected terrain comprise an area of about 60 990 km^2 or 28% of the quartiles, whereas shallow slides and gullied terrain affect only 16% of the quartiles. RTS-affected quartiles has an 81% correspondence with aerial survey observations (Table 2).

The broad-scale hillslope thermokarst landscape coverage from Olefeldt et al. (2016) indicates a significant departure from the TMC distribution of RTS, indicating only 12% overall correspondence (Figs. 7D and 7E, and Table S4Ai). The overall poor agreement relates mainly to the prediction of sensitive slopes or relict ice over large areas where no RTS were observed (Table S4Aii). The agreement between TMC-derived RTS-affected terrain and categories of relict ice abundance (O'Neill et al. 2022) is about 41% (Figs. 7D and 7F; Table S4Ai); however, several RTS hotspots in ice-marginal moraine are modelled as having high relict ground ice abundance (O'Neill et al. 2022). Both modelled products identify western Arctic Canada as being broadly thaw sensitive, with 83% and 41% of the TMC mapped RTS-affected grid cells occurring in moderate-to-high hillslope thermokarst sensitivity and relict ground abundance, respectively.

The mapped terrain affected by ice-wedge polygons (IWP) in uplands east of the Mackenzie Delta shows a 69% correspondence with polygon fields mapped by air photo interpretation (Lantz et al. 2017) (Figs. 8A–8C and Table 1A). These spatial datasets show an increasing northward trend in the abundance of polygonal terrain reflecting colder winter ground temperatures, frequent thermal contraction cracking, and larger, more widespread ice-wedge networks in the tundra than in the subarctic (Kokelj et al. 2014). Distinct areas of higher and lower polygonal terrain density in both datasets reflect variations in the abundance of lacustrine deposits that host polygonal peatlands (Fig. 1Biii) (Steedman et al. 2017). For the entire western Arctic region, polygonal terrain-affected grid cells have a 96% correspondence with aerial survey observations (Fig. 8D and Table 2).

Polygonal terrain occurs at high abundances in low- and mid-Arctic environments and decreases across the forest–tundra transition (Fig. 8D). The complex patterns of polygonal terrain distribution mapped by the TMC reflect variations in wedge ice abundance in conjunction with landscape types where polygon expression is best visible on Sentinel-2 imagery. Notably, the TMC identified polygonal terrain in the Mackenzie Delta, southwest of Inuvik, where ice-wedge networks are expressed by patterned forest (Kokelj and Burn 2004), high abundance was mapped across the ice-wedge-rich unglaciated Tuktoyaktuk Coastal lowland (Rampton 1988), and the greatest abundances were observed in association with ice-cored moraine around Paulatuk and along the

Fig. 7. (A) Map of terrain affected by active retrogressive thaw slumps (RTS) on Banks Island from the Northwest Territories (NT) Thermokarst Mapping Collective (TMC) project. (B) Point data showing RTS occurrences from Lewkowicz and Way (2019) and (C) converted to raster data for comparison with (A). (D) TMC data showing terrain affected by RTS, western Arctic Canada (215 426 km²), inset (E) is modelled slope thermokarst terrain from Olefeldt et al. (2016), and (F) is modelled potential of relict ground ice occurrence from O'Neill et al. (2022). The water layer is from the National Hydro Network (Natural Resources Canada 2016) and the hill-shaded topography is from the Canadian Digital Elevation Model (Natural Resources Canada 2015). The map projection is NAD 83, NWT Lambert.
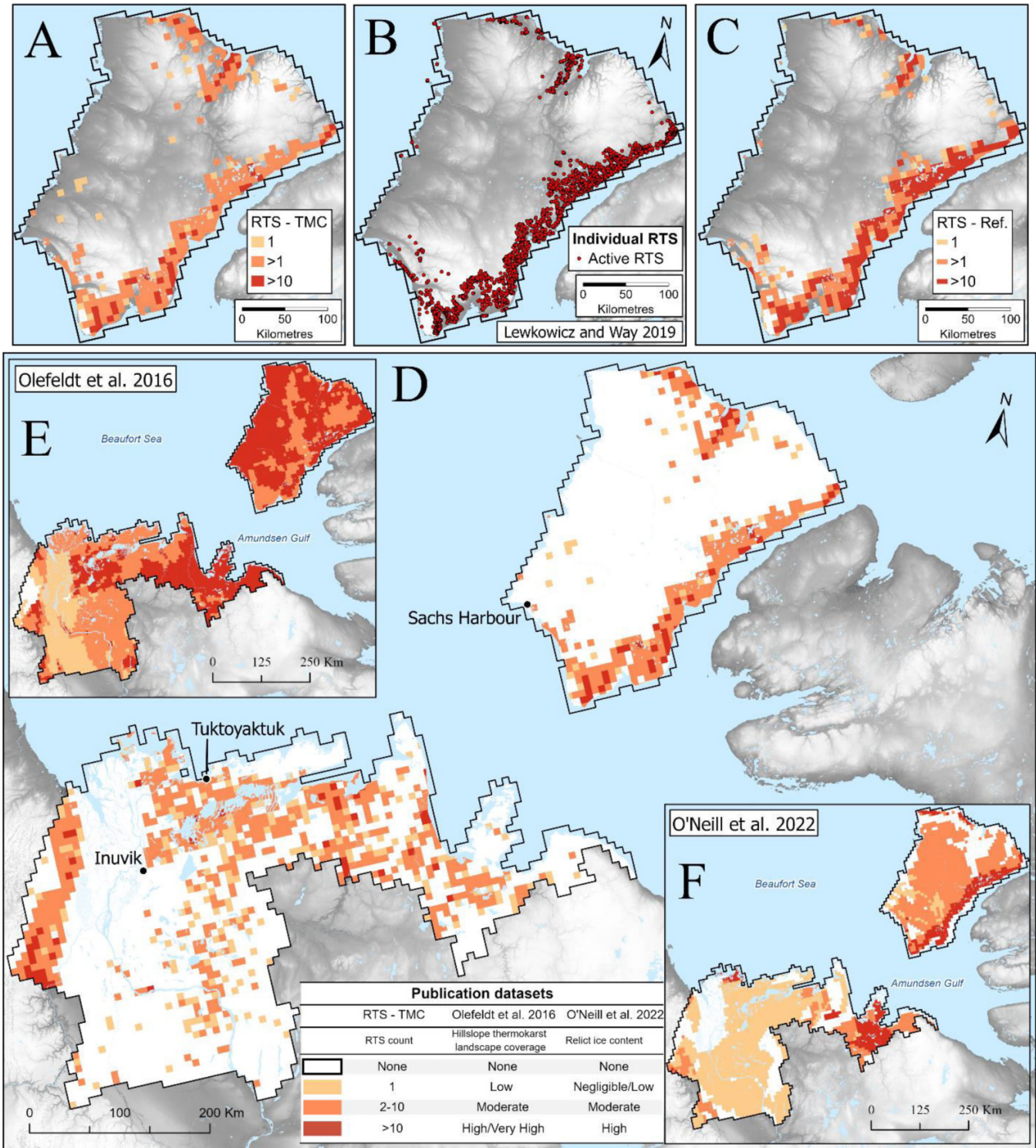
Table 1. (A) Summary of accuracy assessments comparing Thermokarst Mapping Collective (TMC) inventory results with independent, fine-scale mapping (reference) datasets for retrogressive thaw slumps (RTS) on Banks Island (Lewkowicz and Way 2019), polygonal terrain in the Tuktoyaktuk Coastlands (IWP) (Lantz et al. 2017), and ramparted lake–lithalsa complexes (RL–L) in the Great Slave Lowlands (Morse and Rudy 2022). (B) Detailed breakdown of comparisons between reference datasets and classified categories. Agreement counts are in bold.

(A)

Feature/attribute	Reference dataset	Agreement total	Reference total	Agreement
Retrogressive thaw slumps	Lewkowicz and Way 2019	1190	1409	84%
Ice-wedge polygons	Lantz et al. 2017	74	107	69%
Ramparted lake–lithalsa complex	Morse and Rudy 2022	41	53	77%

(B)

Feature/attribute	Classified dataset	Reference dataset	Reference category	Classified category				Total reference grid cells	Agreement
				None	Low	Moderate	High		
Retrogressive thaw slumps	TMC-RTS	Lewkowicz and Way 2019	None	**1051**	22	37	2	1112	95%
			Low	28	**8**	10	0	46	17%
			Moderate	17	8	**91**	4	120	76%
			High	1	0	90	**40**	131	31%
				Negligible	Low	Moderate			
Ice-wedge polygons	TMC-IWP	Lantz et al. 2017	Negligible	**43**	20	1		64	67%
			Low	8	**31**	4		43	72%
			Moderate	0	0	**0**		0	0%
				None	Trace	Abundant			
Ramparted lake–lithalsa complex	TMC-LR–L	Morse and Rudy 2022	None	**0**	1	0		1	0%
			Trace	3	**22**	4		29	76%
			Abundant	0	4	**19**		23	83%*

*See Table S2 for normalization of reference datasets to enable comparisons with TMC inventory data.

Table 2. Correspondence of Thermokarst Mapping Collective (TMC) grid cell classification with the 2020–2022 oblique aerial inventories of thermokarst landforms for retrogressive thaw slumps (RTS) and ice-wedge polygons (IWP) across the western Arctic region and ramparted lake–lithalsa complexes (RL–L) in the Taiga Plains and Taiga Shield, north of Great Slave Lake.

|	Feature/attribute		
	RTS	IWP	RL–L
Overlapping quartiles	251	226	73
Missed quartiles	47	9	19
Confirmed observations	204	217	54
Agreement	81%	96%	74%

Note: Confirmed observations occur when an oblique aerial observation of specific phenomena was identified by the TMC mapping for a specific grid cell. Missed grid cell indicates that an oblique aerial observation was not captured by the TMC.

northeast-trending bands of moraine on the northwest and southeast sides of Banks Island (Fraser et al. 2018). The distribution of IWP-affected terrain from the TMC is reflected by general patterns in modelled abundance of wedge ice from O'Neill et al. (2022) (Fig. 8E); however, detailed inspection reveals contrasts that result in a low agreement between the datasets (Table S4Bi). The circumpolar-scale statistical modelling of environments suitable for IWP from Karjalainen et al. (2020) was developed to assess climate change impacts on

the distribution of these features. The majority of disagreement occurs because Karjalainen et al. (2020) modelled little variation in high IWP suitability across most of the terrain that the TMC inventory indicates has variable IWP abundance, producing large "errors" of commission (Figs. 8D and 8F, and Table S4Bii).

The distribution of terrain affected by thermokarst lakes and ponds that develop in ice-rich glaciolacustrine deposits of the Great Slave Lowlands was mapped by the TMC project (Fig. 9A). These thermokarst lake environments are referred to here as "RL–L complexes" following descriptions in Wolfe and Morse (2017) and Morse et al. (2017) (Fig. 1Ci). There is a 77% agreement between the TMC product and summarized data derived from high-resolution satellite imagery from Morse and Rudy (2022) (Figs. 9A–9C and Table 1A), and 74% correspondence between grid-based identification of RL–L complexes and aerial survey observations over the larger North Slave Region (Fig. 9D and Table 2). Regional patterns over an area of 51 968 km^2 indicate that the highest abundance of RL–L complexes occurs adjacent to Great Slave Lake, where ice-rich glaciolacustrine sediments are widespread. These thaw-sensitive thermokarst lake environments decrease in abundance with increasing elevation and distance from the lake as fine-grained deposits diminish and the landscape becomes increasingly bedrock-dominated (Fig. 9D). The patterns of modelled segregated ice abundance (Fig. 9E) (O'Neill et al. 2022) show reasonable agreement with mapped thermokarst lake landforms (55%) (Table S4Ci). The

Fig. 8. (A) Map showing the abundance of polygonal terrain across tundra uplands east of Mackenzie Delta from the Northwest Territories (NT) Thermokarst Mapping Collective (TMC) project. (B) Digitized ice-wedge polygonal terrain from Lantz et al. (2017) and (C) converted to raster data for comparison with (A). (D) TMC data showing the distribution of polygonal terrain for western Arctic Canada (215 469 km²), inset (E) is modelled wedge ice abundance from O'Neill et al. 2022; and (F) is modelled potential environmental space for the occurrence of ice-wedge polygons (IWP) from Karjalainen et al. (2020). The water layer is from the National Hydro Network (Natural Resources Canada 2016) and the hill-shaded topography is from the Canadian Digital Elevation Model (Natural Resources Canada 2015). The map projection is NAD 83, NWT Lambert.
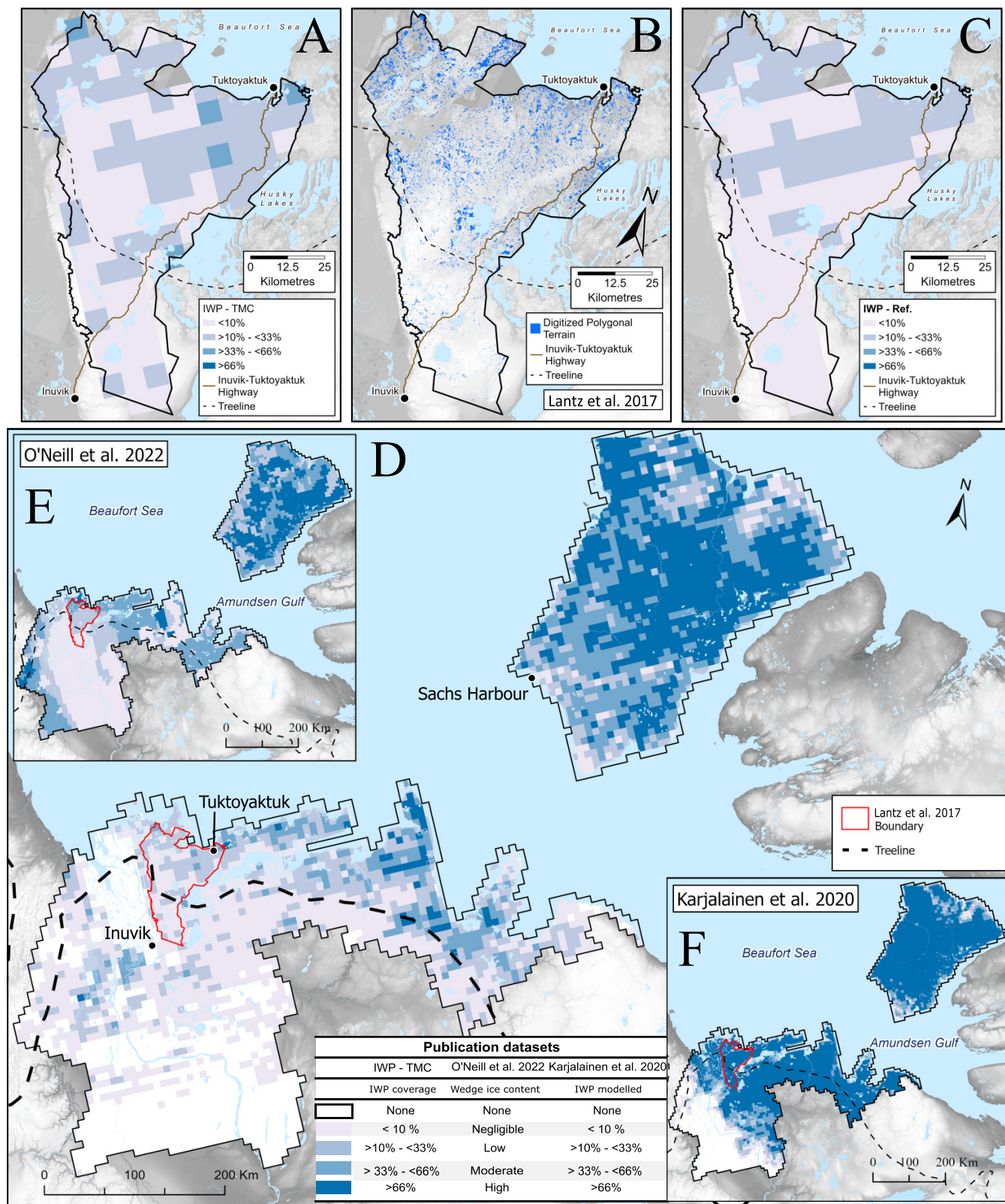
Fig. 9. (A) Map showing the abundance of ramparted lake–lithalsa (RL–L) complexes from the Northwest Territories (NT) Thermokarst Mapping Collective (TMC) project. (B) Point data of individual lake–lithalsa complexes from (Morse and Rudy 2022), and (C) the summary of these data on a raster framework for comparison with (A). (D) Broad-scale map showing the distribution of lake lithalsa complexes for a 51 968 km² area of the Taiga Shield and Taiga Plain ecoregions from the TMC. (E) The modelled potential abundance of segregated ice from O'Neill et al. (2022) and (F) terrain susceptible to lake thermokarst from Olefeldt et al. (2016). The water layer is from the National Hydro Network (Natural Resources Canada 2016) and the hill-shaded topography is from the Canadian Digital Elevation Model (Natural Resources Canada 2015). The map projection is NAD 83, NWT Lambert.
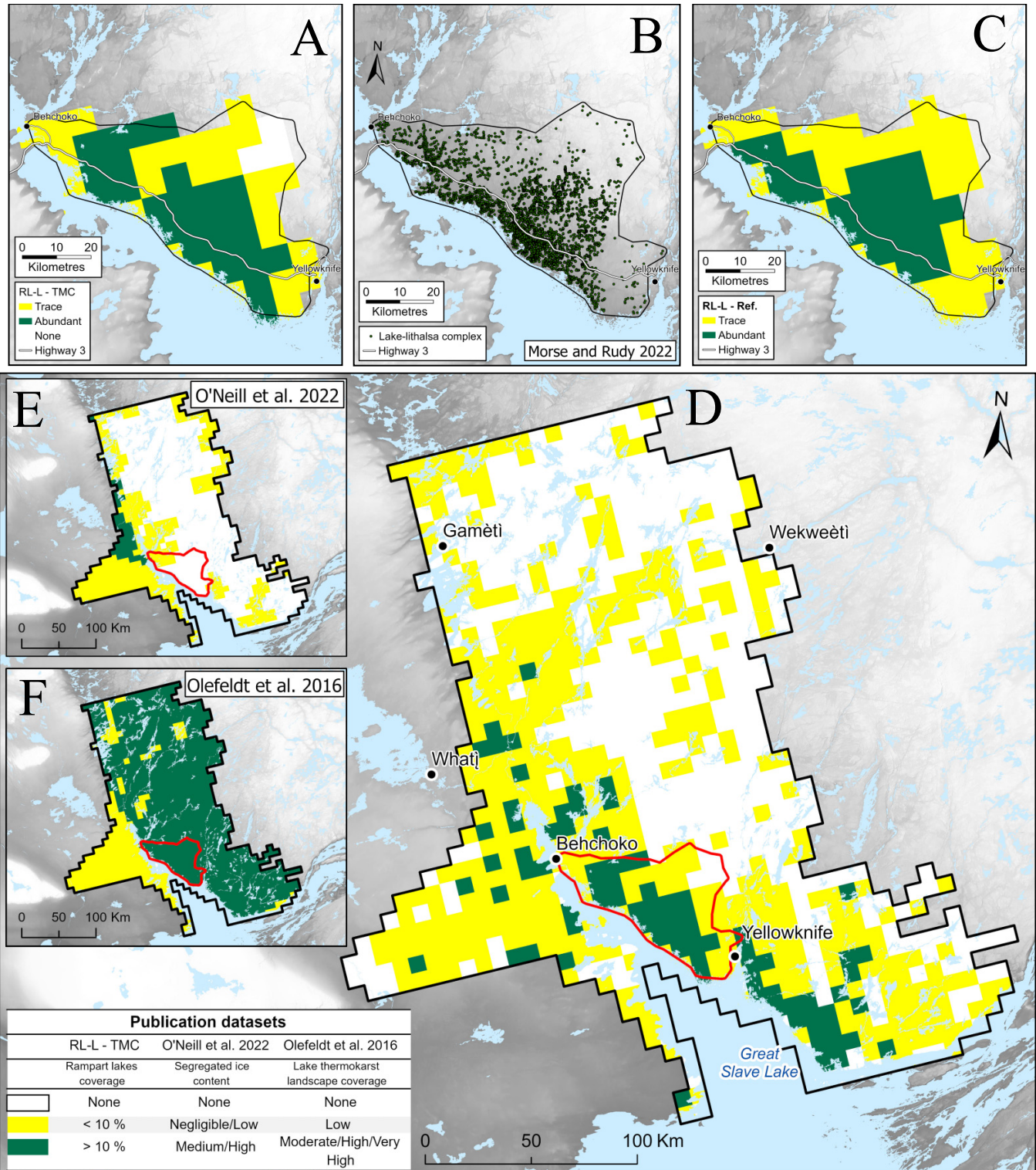
coarse–resolution surficial geology data used in the modelling indicates mainly bedrock in the region, explaining why segregated ground ice was not predicted in several areas of abundant thermokarst lake observations (Figs. 9D and 9E, and Table S4Cii). Appreciable fine-grained, frost-susceptible deposits are mapped in more detailed surficial geology products (Kerr et al. 2022), and their use would likely improve modelling outputs (O'Neill et al. 2022). Moderate-to-high density of thermokarst lake-affected landscapes were projected to occupy 77% of this study domain by a circumpolar assessment of thermokarst-sensitive terrain (Olefeldt et al. 2016) (Fig. 9F); however, the empirical mapping of this bedrock-dominated environment indicates that only about 9% of the area hosts moderate-to-high amounts of thermokarst lakes. In contrast with the possible underprediction of segregated ice abundance, the modelled thermokarst lake terrain has a poor agreement with the TMC mapping due to large errors of commission (Table S4Cii).

4.2. Quantifying the "thermokarst fingerprint" of a landscape

Here, we show that the holistic nature of the TMC inventory captures differences in thermokarst and periglacial characteristics across landscapes with contrasting permafrost, geomorphic, and Quaternary paleoenvironmental conditions (Fig. 10). We compared Eastern Banks Hills in the mid-Arctic region and the Tuktoyaktuk Coastal Plain in the southern Arctic region, both underlain by ice-rich glacial deposits and continuous permafrost, with the Great Slave Lowland within the Precambrian Shield and discontinuous permafrost zone where ice-rich terrain is limited to low-lying areas with glaciolacustrine deposits (Figs. 2 and 10).

Eastern Banks Hills and the Tuktoyaktuk Coastal Plain comprise landscape units widely affected by retrogressive thaw slumping (76% and 80%, respectively). In addition, 29% of the cells in the fluvially incised ice-cored environments of the Eastern Banks Hills are affected by larger (approximately >400 m) thaw-driven disturbances with debris tongues entering water bodies we term "mega slumps", and 28% of the mapping units also have smaller shallow slides. Thaw-driven mass wasting features are not observed in the low relief and bedrock-dominated Great Slave Lowland. Hydrological features indicating thaw-sensitive terrains are similar between the two northern ecoregions. For example, shorelines affected by RTS occur in about half of the grid cells in each of the northern regions, with only limited evidence of recent lake expansion or lowered lake levels (recent drying or drainage).

Notable differences exist between the two northern regions regarding the nature and distribution of wedge ice. Polygonal terrain and polygonal-patterned ponding are observed across both environments; however, they are ubiquitous across the Eastern Banks Hills. On Banks Island, the top-down thaw of large ice wedges across upland terrain identified by polygonal-patterned pond expansion is also widespread, occurring at greater than trace amounts in 60% of the affected grid cells (Fraser et al. 2018). Ice-wedge thermokarst was detected at only trace amounts in 13% of the grid cells over the Tuktoyaktuk Coastal Plain, though recent top-down thaw and subsidence of hillslope ice-wedge troughs have been observed by field monitoring at Illisarvik just to the north of the mapped ecoregion (Burn et al. 2021). In contrast to the two Arctic ecoregions, the dominant indicator of thermokarst–hydrology interactions in the Great Slave Lowland manifests as RL–L complexes common throughout ice-rich glaciolacustrine deposits and observed in over 60% of the quartiles (Figs. 1Ci, 9, and 10) (Wolfe and Morse 2017; Morse and Rudy 2022). These landforms are also commonly characterized by thermokarst ponding or by dry basins, suggesting that water levels have lowered, which were observed in 31% and 34% of the grid cells, respectively.

In the periglacial theme, the Eastern Banks Hills are characterized by widespread polygonal terrain. In the ice-rich Tuktoyaktuk Coastal Plain, polygonal terrain is most common throughout the lowlands, which also host abundant pingos (Wolfe et al. 2023) detected in 72% of the quartiles. Involuted topography indicating ice-cored terrain (Dallimore et al. 1996) was observed in 61% of the grid cells in the Tuktoyaktuk Coastal Plain but is absent from Eastern Banks Hills. In contrast with the two northern ecoregions, this suite of periglacial landforms was not observed in the Great Slave Lowland. All three ecoregions are characterized by terrain with thick organic soils, which occurs in most grid cells on Eastern Banks Hills and is mainly restricted to small pockets (trace = 89%). In the Great Slave Lowland, peat-rich terrain was identified in 45% of the quartiles, mostly occurring as discrete features. In the Tuktoyaktuk Coastal Plain, terrains with thick organic soils are widespread and occur over larger portions of the landscape in 45% of the quartiles where lacustrine basins host extensive polygonal peat plateaus (Steedman et al. 2017). There was little evidence of degradation in northern peatlands, whereas greater than trace amounts of degradation was observed in most of the grid cells with organic terrains in the Great Slave Lowlands.

5. Discussion

To our knowledge, this is the first empirically based permafrost mapping project of this nature and scope. Here, we summarize outputs and anticipated outcomes of this project, which highlights the implications, challenges, and opportunities that shaped the approaches and methods.

5.1. The importance of empirical data on the distribution and diversity of permafrost landforms

As permafrost landscapes change with climate warming and the abundance of modelled or remotely sensed spatial products increases, a heightened need exists for empirically based permafrost data to generate new knowledge and test model outputs. Comparisons with independent data demonstrate the effectiveness of TMC outputs in depicting thermokarst landforms or thaw-sensitive terrain. For example, the inventory of landscapes affected by RTS, IWP terrain, and RL–L (thaw lake) complexes show good agreement with fine-scale spatial datasets (10^2–10^4 km^2) (Table 1; Figs. 7A–7C,

Fig. 10. The thermokarst fingerprints of different permafrost landscapes are shown through the summary of landscape or feature occurrence grouped by mapping theme for Level IV ecoregions from (A) mid-Arctic (East Banks Hills), (B) southern Arctic (Tuktoyaktuk Coastal Plain), and (C) Taiga Shield (Great Slave Lowland). From top to bottom, the data are the percentage of quartiles within an ecoregion with evidence of the respective features or landscape types. The shading of the bars differentiates the percentage of the grid cells where observation was in trace (<10%) or greater than trace (>10%) abundance. For features with counts, trace refers to a single observation within a grid cell.
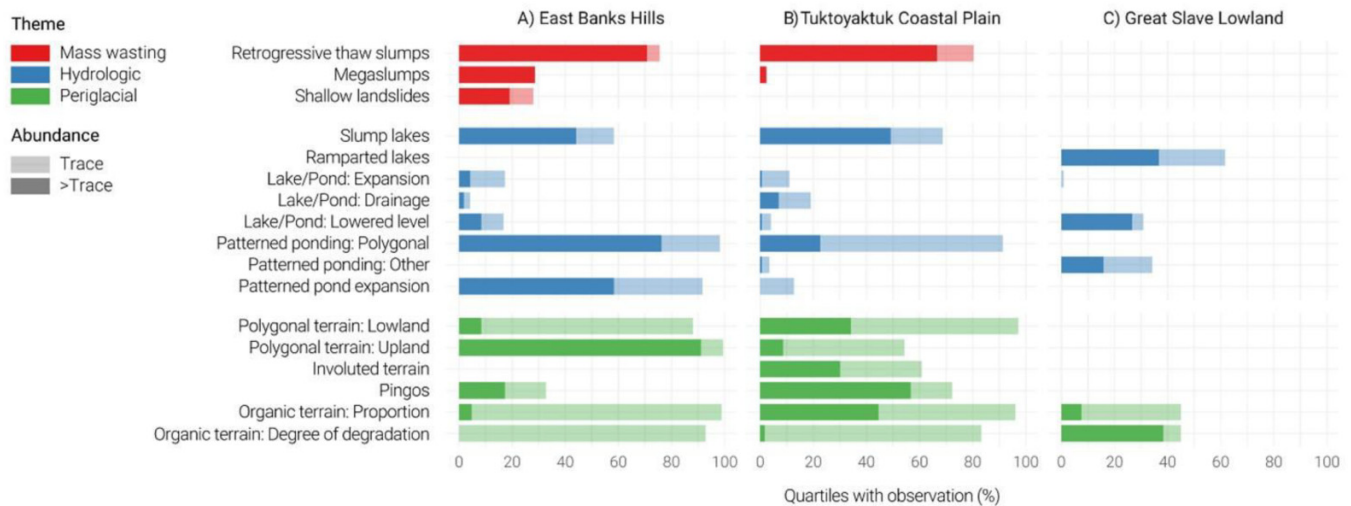
8A–8C, and 9A–9C) and correspondence with aerial inventories of thermokarst and periglacial features over larger areas (10^4–10^5 km^2) (Table 2). The spatial data products developed by the TMC are valuable indicators of thaw-sensitive terrain (Figs. 7–9), so we compared them to broad-scale spatial data products that depict thermokarst landscapes and modelled ground ice abundance. We recognize the inherent differences between the empirical TMC spatial products, which portray observed phenomena and the modelling outputs where statistical or rule-based schemes were integrated through geomatics procedures to depict landscape susceptibility, likelihood of occurrences, or relative abundances. Regardless, we show significant deviations and some notable similarities between TMC and recent broad-scale maps (Figs. 7–9 and Table S4) highlighting the importance of empirically derived data for evaluating spatial modelling and remote sensing products, and generating new information on the distribution and diversity of thaw-sensitive permafrost terrain at regional to global scales.

The low agreement between several TMC data outputs and broad-scale synthesis products depicting the sensitivity of permafrost terrain underlines the risk with their application in regional-scale land use planning and decision-making, and for extrapolating local-scale field measurements to produce regional or circumpolar-scale summaries. Often, our basic theme-specific comparisons showed that differences of omission characterized the comparison with one modelled product, and differences of commission characterized the other (Figs. 9D–9F; Table S4Cii). A more rigorous empirical evaluation of model outputs is necessary to understand their limitations, inform the improvement of rule-based assumptions or input data layers used in spatial modelling, and

focus on the production of robust regional-scale validation datasets (Wang et al. 2023). Our comparisons are also useful reminders that the application of these broad-scale spatial data products should be limited to showcasing general patterns and relevance of thaw-driven processes on terrain, ecosystems, carbon release, and infrastructure (Olefeldt et al. 2016; Chadburn et al. 2017; Hjort et al. 2018; O'Neill et al. 2022). Since these rule-based spatial products insufficiently represent (i) the heterogeneity in permafrost, soil, ground thermal, and terrain conditions, (ii) variation in climate drivers that yield a diverse array of landforms, and (iii) thaw-driven landscape responses, their use in prediction or decision-making is cautioned. Conceptual models provide a useful framework to connect geological legacies and paleoenvironmental history with the nature and occurrence of ground ice or thermokarst processes and landforms (O'Neill et al. 2019), but their implementation through broad-scale maps is constrained by the quality and resolution of existing geospatial data and the current state of permafrost–landscape knowledge. The integration and syntheses of fine-scale depictions of thaw-sensitive terrain can also be challenging because most datasets are necessarily limited in spatial extent, describe a narrow range of landforms (Steedman et al. 2017; Lewkowicz and Way 2019; Wang et al. 2023), and the methods and outputs vary because they are tailored to specific project needs and questions. Our development of systematic, empirically derived spatial datasets that quantify thermokarst and periglacial landform distribution for the permafrost regions of northwestern Canada addresses a foundational data and knowledge gap through initiating a more robust characterization of thaw-sensitive terrain over broad-spatial scales.

The depth of the TMC dataset also highlights that climate-driven permafrost thaw comprises a wide range of processes and landforms that manifest in complex combinations across the landscape. Recognizing the need to develop geomorphically based conceptual frameworks of permafrost thaw supported by more holistic approaches to quantifying thaw-driven landscape change, the TMC project data model and methods describe the variable nature of thermokarst and thaw-sensitive landscapes (Figs. 1, S1, and S2). The results demonstrate that this systematic inventory captures the diversity of permafrost terrain conditions within and between ecoregions, which can be described by their contrasting permafrost characteristics or *thermokarst fingerprints* (Fig. 10), providing novel datasets to explore variation in thaw-driven consequences on northern environments and society.

5.2. Northern science capacity and collaboration

The TMC is guided by the science priorities of a northern-based team that leveraged the expertise of Federal and academic research partners to improve knowledge of the nature and distribution of thaw-sensitive permafrost terrain in the NT. Northern-driven permafrost science initiatives are rare in Canada because the capacity to conceptualize and implement research and monitoring programs has traditionally rested in southern institutions. The evolution of Territorial and Indigenous governance has stimulated policies to strengthen northerners' roles in Arctic science (Inuit Tapiriit Kanatami 2018; National Geological Surveys Committee 2022), and the growth of northern-based research organizations has facilitated opportunities for science collaboration and co-developing knowledge (Thompson et al. 2020). The Territories' investment in permafrost technical capacity has actioned science strategies (GNWT 2018) and enabled research partnerships to be leveraged through more equitable collaborations that address northern priorities. A key government–university partnership, the GNWT–WLU agreement, has also provided a framework and flexibility to co-manage a Yellowknife-based TMC project coordinator position. Critical support to the development, and rigor of technical products and outputs (e.g., Gibson et al. 2021; Wolfe et al. 2022) has been the sustained commitment of Federal and academic research partners. Based on our collective experience, we emphasize that developing permafrost knowledge collaboratively *with* northern partners can increase project relevance and accountability, build scientific and technical capacities, strengthen relationships with Indigenous partners and practitioners, and increase the likelihood that research outputs will be understood and applied in northern planning and decision-making.

5.3. Strengthening relationships with northerners

Ongoing outreach has helped to identify a diverse range of northern needs, inform our approaches, prioritize mapping, and foster new partnerships. For example, the NWT Association of Communities emphasized the need for better information on the effects of permafrost thaw, and so the TMC prioritized the mapping and synthesis of permafrost sensitivity for NT communities and has presented results at related northern workshops and conferences (Table S5). The Territorial Lands and Infrastructure Departments have worked with the TMC to adopt mapping and aerial assessment methods over liabilities and infrastructure corridors. The TMC project framework, methods, and spatial data provide an entry point to foster the discussion about permafrost terrain sensitivity, community concerns, and land management needs. Relationships with Indigenous partners facilitated through projects or programs with established community linkages have created opportunities for information sharing, and the development or renewal of partnerships (Table S5). For example, the presentation of methods and maps at workshops with the Inuvialuit Land Administration, Łı́ı́dlı̨ Kú̧ę́ First Nation, and K'asho Got'ı̨nę Foundation have supported fieldwork collaboration, discussions on permafrost-driven landscape change, areas of community interest, and the development of monitoring programs led by Indigenous Guardians and Land Management organizations. The project has fostered discussions around permafrost issues to strengthen the capacity of these partners through training, implementation of methods for fine-scale mapping and monitoring, and collaboration on aerial validation activities, and in turn gained insights on observations of change and research priorities. A new linkage has been established with the Gwich'in Land Use Planning Board who have gained some capacity to manage spatial data, conduct mapping, and leverage preliminary spatial data products from the project to support land use planning. A common constraint in effective science collaboration relates to capacity limitations of many northern partners, and the time and resources required by researchers to listen and develop spatial datasets that meet partner needs.

5.4. Geomatics capacity and SDI (technical realities)

The project adopted a low-cost, user-centered solution (Fig. 6) that facilitated the exchange of geospatial data and services between mappers and researchers situated in different organizations across Canada (Hjelmager et al. 2008; Michener 2015) and allowed for design modifications as information and performance requirements evolved. This required geomatics capacity via a project coordinator who developed and maintained an SDI that could address data management and mapping needs. Effective communication between the coordinator and researchers was critical, ensuring that the SDI accounted for the capacity and resource limitations inherent in northern organizations, and maintained the flexibility required to support an evolving database and a growing number of collaborators in a decentralized mapping framework (Figs. 3 and 5).

A file-based architecture was necessary during the project's development phase but had demonstrated inadequacies as the number of users and requirements for quality control increased. For example, managing and merging overlapping edits in the master database required automated data quality assessments and updating, which became increasingly inefficient as the number of mappers increased, (García-Chapeton

et al. 2018). An enterprise GIS system, which enables simultaneous database access by multiple users and automated updates, could improve efficiency but it requires reliable internet connections to remote servers, high annual subscription fees, and resources to support database and infrastructure management (Keating et al. 2003; Kong 2015; Coetzee et al. 2017; Esri 2022). Government partners have enterprise GIS functionality, but the implementation cycles and security requirements would have hindered project development and collaboration across institutions. While these issues were resolved by implementing a user-centered design (Fig. 6B), recent advances in cloud computing and remote servers provide efficient solutions for facilitating a decentralized–synchronous collaboration (García-Chapeton et al. 2018), overcoming SDI limitations that have challenged small organizations. Looking forward, these new tools have the potential to support decentralized, northern-focused research collaborations; however, GIS capacity will still be required for their implementation.

5.5. Flexibility and perseverance

The implementation and progress of the TMC required perseverance, adaptability, and sustained commitment from a network of experts across NT and Canada. The decentralized approach and flexible organizational structure (Figs. 3 and 6) enabled iterative design, adaptation to changes in funding, accommodation of new stakeholder interests, and progress throughout the COVID-19 pandemic and onward. This project environment permitted revisions to scope and schedules and integration of new ideas. The growing connections with stakeholders and multiyear vision facilitated a stepwise approach with initial emphasis on documenting scientific methods, recruiting and training mappers, generating data, and validating results with field/aerial observations. Gradual progress has led to some changes in participants; however, the commitment of core contributors and organizations has maintained momentum (Fig. 3). The institutional support from the Territorial Government through enhancing northern-based permafrost capacity has enabled multiyear project planning, offsetting the limitations of short-term funding cycles typical of funding in academia (Pulsifer et al. 2011). This project has matured as feasibility and value was realized and communicated to partners and stakeholders through ongoing discussions and outreach (Table S5). For very large or centrally funded projects with rigid timelines and strict definitions of collaborators and scope, or in research environments where rapid publication defines success, the TMC approach would not be feasible.

6. Summary and looking ahead

This study documents the development, implementation, and progress of a northern-driven project where permafrost researchers across Canada worked collaboratively to produce an empirically based inventory of thermokarst terrain and indicators of permafrost thaw sensitivity for the NT. This project addresses a foundational information gap on the distribution of thaw-sensitive permafrost terrain through collaboration and co-development of permafrost knowledge. It

was made possible by growth of northern permafrost capacity, sustained collaboration with government, academic and Indigenous partners, and core geomatics capacity that enabled development and implementation of the SDI necessary to support a decentralized mapping approach. Documentation of methods by expert teams supported mapper training, and the flexible data infrastructure has facilitated the continued engagement of research partners across Canada in generating data products through the COVID-19 pandemic. Project communications through ongoing dialogue with northern stakeholders and data sharing with land use planning boards has strengthened linkages, informed design, and fostered new partnerships.

The TMC approach is enabling rapid NT-wide landscape assessments of 25 thermokarst and periglacial features. The mapping outputs are well validated against independent data and when complete will provide the first comprehensive coverage describing variation and diversity of permafrost terrain types for a 2 million km^2 region of northern Canada. Our comparisons with broad-scale spatial products demonstrate that TMC provides new quantitative information on the distribution of thaw-sensitive permafrost terrain that can be used to evaluate spatial modelling products. The approach and resulting datasets provide a holistic framework to explore the diversity and trajectories of thaw-driven change, advance spatial modelling through the development of training and validation datasets, and engage partners in generating regional or community-based syntheses that explore what permafrost thaw means for Canada's changing North.

Acknowledgements

oblique photo dataset. Access to Inuvialuit, Gwich'in, Łı́ı́dlı̨ Ku̱ʼeʼ, and K'asho Got'ı̨nę lands is gratefully acknowledged. Constructive comments from two anonymous reviewers have improved the quality of this manuscript. NTGS contribution #0152.

Article information

Copyright

Data availability

The datasets and sources used in this publication are indicated in figure captions and Table S1. All methodological guides and project-related data products are being made available through the NTGS Open Report publication system or through the NWT Centre for Geomatics (e.g., Gibson et al. 2021; Wolfe et al. 2022). The oblique photo dataset can be accessed via public REST Service Endpoint: https://www.apps.geomatics.gov.nt.ca/arcgis/rest/services/GNWT_Operational/NTGS_ThermokarstCollective_Operational/MapServer. Given the breadth and scope of the TMC project, the preliminary nature of the datasets presented in this paper, and additional methodological reports in review or in preparation, materials, and data can be provided upon request, and will be found at the NTGS Open Report system or in other open data repositories that will be cross-referenced with this overview paper.

Author information

Author ORCIDs
Steven V. Kokelj https://orcid.org/0000-0002-2840-2605
Peter D. Morse https://orcid.org/0000-0003-3740-2022
Stephen A. Wolfe https://orcid.org/0000-0001-7255-1184
Jurjen van der Sluijs https://orcid.org/0000-0002-9244-1756
Niels Weiss https://orcid.org/0000-0001-8905-343x
H. Brendan O'Neill https://orcid.org/0000-0002-5290-3389
Jennifer L. Baltzer https://orcid.org/0000-0001-7476-5928
Trevor C. Lantz https://orcid.org/0000-0001-5643-1537
Alexandre Chiasson https://orcid.org/0000-0003-1852-0138
M. Alice Wilson https://orcid.org/0000-0002-0376-0158
Joseph M. Young https://orcid.org/0000-0002-8917-0078

Author contributions
Conceptualization: SVK, PDM, SAW, JvdS, TCL, JLB, RHF
Data curation: SVK, TG-H, SVD, NW, JvdS, CF, CG
Formal analysis: SVK, TG-H, SVD, ACAR, JvdS, NW, CF
Funding acquisition: SVK, PDM, JLB, TCL, DC, DGF, GG, CK, SFL, WLQ, MRT
Investigation: SVK, TG-H, SVD, PDM, SAW, JvdS, NW, HBO, TCL, CG, AC, CF, MN, MP, JAP, MAW, JMY
Methodology: SVK, TG-H, PDM, SAW, ACAR, JvdS, HBO, TCL, CG, RHF, SFL, MRT, AC, CF, MP, JAP, MAW, JMY
Project administration: SVK, TG-H, SVD, ACAR, JLB, TCL, DC, GG, CK, WLQ
Resources: SVK, PDM, JLB, TCL, DGF, GG, CK, SFL, WLQ, MRT
Software: TG-H, SVD, JvdS
Supervision: SVK, PDM, SAW, JvdS, JLB, TCL, DC, DGF, GG, SFL, WLQ, MRT
Validation: SVK, TG-H, SVD, JvdS, HBO, RHF, JAP
Visualization: SVK, TG-H, SVD, PDM, JvdS, NW, HBO
Writing – original draft: SVK, TG-H
Writing – review & editing: SVK, TG-H, SVD, PDM, SAW, HBO, ACAR, JvdS, JLB, TCL, MRT, AC, JMY, RHF, WLQ

Competing interests
The authors declare that there are no competing interests.

Supplementary material

Supplementary data are available with the article at https://doi.org/10.1139/AS-2023-0009.

References

Allard, M., L'Herault, E., Aube-Michaud, S., Carbonneau, A., Mathon-Dufour, V., St-Amour, A.B., and Gauthier, S. 2023. Facing the challenge of permafrost thaw in Nunavik communities: innovative integrated methodology, lessons learnt, and recommendations to stakeholders. Arctic Science. doi:10.1139/AS-2022-0024.

Aylsworth, J.M., and Kettles, I.M. 2000. Distribution of peatlands. *In* The physical environment of the Mackenzie Valley, Northwest Territories: a base line for the assessment of environmental change. *Edited by* L.D. Dyke and G.R. Brooks). GSC Bulletin 547. pp. 49–55.

Aylsworth, J.M., Duk-Rodkin, A., Robertson, T., and Traynor, J.A. 2000. Landslides of the Mackenzie Valley and adjacent mountainous and coastal regions. *In* The physical environment of the Mackenzie Valley, Northwest Territories: a base line for the assessment of environmental change. *Edited by* L.D. Dyke and G.R. Brooks). Geological Survey of Canada, Bulletin 547. pp. 167–176.

Biskaborn, B.K., Smith, S.L., Noetzli, J., Matthes, H., Vieira, G., Streletskiy, D.A., et al. 2019. Permafrost is warming at a global scale. Nature Communications, **10**: 264. doi:10.1038/s41467-018-08240-4. PMID: 30651568

Brardinoni, F., Scotti, R., Sailer, R., and Mair, V. 2019. Evaluating sources of uncertainty and variability in rock glacier inventories. Earth Surface Processes and Landforms, **44**: 2450–2466. doi:10.1002/esp.4674.

Brown, J., Ferrians, O.J., Heginbottom, J.A., and Melnikov, E.S. 2002. Circum-Arctic map of permafrost and ground-ice conditions, version 2 [data set]. National Snow and Ice Data Center, Boulder, CO. doi:10.7265/skbg-kf16.

Burn, C.R., Lewkowicz, A.G., and Wilson, M.A. 2021. Long-term field measurements of climate-induced thaw subsidence above ice wedges on hillslopes, western Arctic Canada. Permafrost and Periglac Process, **32**: 261–276. doi:10.1002/ppp.2113.

Bush, E., and Lemmen, D.S. (*Editors*). 2019. Canada's Changing Climate Report. Government of Canada, Ottawa, ON. p. 444.

Calmels, F., Laurent, C., Brown, R., Ireland, M., Marie, J., First, R., and River, J.M. 2015. How permafrost thaw may impact food security of Jean Marie River First Nation, NWT. *In* 68th Conférence Canadienne de Géotechnique et 7th Conférence Canadienne sur le Pergélisol, 20 au 23 septembre 2015. Québec, QC.

Chadburn, S.E., Burke, E.J., Cox, P.M., Friedlingstein, P., Hugelius, G., and Westermann, S. 2017. An observation-based constraint on permafrost loss as a function of global warming. Nature Climate Change, **7**: 340–344. doi:10.1038/nclimate3262.

Chen, L., and Wang, L. 2018. Recent advance in earth observation big data for hydrology. Big Earth Data, **2**: 86–107. doi:10.1080/20964471.2018.1435072.

Chiasson, A., and Allard, M. 2022. Thermal contraction crack polygons in Nunavik (northern Quebec): distribution and development of polygonal patterned ground. Permafrost & Periglacial Processes, **33**: 195–213. doi:10.1002/ppp.2150.

Chila, Z.K.E., Dunmall, K., Proverbs, T., and Lantz, T.,Aklavik Hunters and Trappers Committee, Inuvik Hunters and Trappers Committee, Sachs Harbour Hunters and Trappers Committee, Olokhaktomiut Hunters and Trappers Committee, and Paulatuk Hunters and Trappers Committee. 2022. Inuvialuit knowledge of pacific salmon range expansion in the western Canadian Arctic. Canadian Journal of Fisheries and Aquatic Sciences, **79**: 1042. doi:10.1139/cjfas-2021-0172.

Chin, K.S., Lento, J., Culp, J.M., Lacelle, D., and Kokelj, S.V. 2016. Permafrost thaw and intense thermokarst activity decreases abundance of stream benthic macroinvertebrates. Global Change Biology, **22**: 2715–2728. doi:10.1111/gcb.13225.

Coetzee, S., Steiniger, S., Köbben, B., Iwaniak, A., Kaczmarek, I., Rapant, P., et al. 2017. The academic SDI—towards understanding spatial data infrastructures for research and education. *In* Lecture notes in geoinformation and cartography. doi:10.1007/978-3-319-57336-6_8.

Cold, H., Brinkman, T., Brown, C., Hollingsworth, T., Brown, D., and Heeringa, K. 2020. Assessing vulnerability of subsistence travel to effects of environmental change in interior Alaska. Ecology and Society, **25**(1): 20. doi:10.5751/ES-11426-250120.

Connon, R., Devoie, É., Hayashi, M., Veness, T., and Quinton, W. 2018. The influence of shallow taliks on permafrost thaw and active layer dynamics in subarctic Canada. Journal of Geophysical Research: Earth Surface, **123**: 281–297. doi:10.1002/2017JF004469.

Dallimore, S.R., Nixon, F.M., Egginton, P.A., and Bisson, J.G. 1996. Deep-seated creep of massive ground ice, Tuktoyaktuk, NWT, Canada. Permafrost and Periglacial Processes, **7**: 337–347. doi:10.1002/(sici)1099-1530(199610)7:4⟨337::aid-ppp232⟩3.0.co;2-3.

Dyke, A.S., and Prest, V.K. 2008. Late Wisconsinan and Holocene history of the Laurentide ice sheet. Géographie physique et Quaternaire, **41**: 237–263. doi:10.7202/032681ar.

Ecosystem Classification Group. 2008. Ecological Regions of the Northwest Territories —Taiga Shield. Yellowknife, NT, Canada. Department of Environment and Natural Resources, Government of the Northwest Territories, Yellowknife, NT. p. 146. Available from https://www.enr.gov.nt.ca/sites/enr/files/wkss_taiga_shield-2008.pdf [accessed 2020].

Ecosystem Classification Group. 2009. Ecological Regions of the Northwest Territories —Taiga Plains. Yellowknife, NT, Canada. Department of Environment and Natural Resources, Government of the Northwest Territories, Yellowknife, NT. p. 173. Available from https://www.enr.gov.nt.ca/sites/enr/files/resources/taiga_plains_ecological_land_classification_report.pdf [accessed 2020].

Ecosystem Classification Group. 2010. Ecological Regions of the Northwest Territories—Cordillera. Yellowknife, NT, Canada. Department of Environment and Natural Resources, Government of the Northwest Territories, Yellowknife, NT. p. 245. Available from https://www.enr.gov.nt.ca/sites/enr/files/resources/cordillera_ecological_land_classfication_report.pdf [accessed 2020].

Ecosystem Classification Group. 2012. Ecological Regions of the Northwest Territories—Southern Arctic. Yellowknife, NT, Canada. Department of Environment and Natural Resources, Government of the Northwest Territories, Yellowknife, NT. p. 170. Available from https://www.enr.gov.nt.ca/sites/enr/files/resources/southern_arctic_ecological_land_classification_report.pdf [accessed 2020].

Ecosystem Classification Group. 2013. Ecological Regions of the Northwest Territories—Northern Arctic. Yellowknife, NT, Canada. Department of Environment and Natural Resources, Government of the Northwest Territories, Yellowknife, NT. p. 157. Available from https://www.enr.gov.nt.ca/sites/enr/files/resources/northern_arctic_ecological_land_classification_report.pdf [accessed 2020].

Esri. 2022. Architecting the ArcGIS platform: best practices. Esri external, Esri, Redlands, CA. pp. 27. Available from https://www.esri.com/content/dam/esrisites/en-us/media/technical-papers/architecting-the-arcgis-system.pdf [accessed 2023].

Fraser, R.H., Kokelj, S. v., Lantz, T.C., McFarlane-Winchester, M., Olthof, I., and Lacelle, D. 2018. Climate sensitivity of high arctic permafrost terrain demonstrated by widespread ice-wedge thermokarst on Banks Island. Remote Sensing, **10**. doi:10.3390/rs10060954.

García-Chapeton, G.A., Ostermann, F.O., de By, R.A., and Kraak, M.J. 2018. Enabling collaborative GeoVisual analytics: systems, techniques, and research challenges. Transactions in GIS, **22**: 640–663. doi:10.1111/tgis.12344.

Gibson, C., Morse, P.D., Kelly, J.M., Turetsky, M.R., Baltzer, J.L., Gingras-Hill, T., and Kokelj, S.V. 2020. Thermokarst Mapping Collective: protocol for organic permafrost terrain and preliminary inventory from the Taiga Plains test area, Northwest Territories. NWT Open Report 2020–010. Northwest Territories Geological Survey, Yellowknife, NT. p. 24. doi:10.46887/2020-010.

Gibson, C., Cottenie, K., Gingras-Hill, T., Kokelj, S. v., Baltzer, J.L., Chasmer, L., and Turetsky, M.R. 2021. Mapping and understanding the vulnerability of northern peatlands to permafrost thaw at scales relevant to community adaptation planning. Environmental Research Letters, **16**: 055022. doi:10.1088/1748-9326/abe74b.

Giuliani, G., Camara, G., Killough, B., and Minchin, S. 2019. Earth observation open science: enhancing reproducible science using data cubes. Data, **4**: 147. doi:10.3390/data4040147.

GNWT. 2018. 2030 NWT Climate Change Strategic Framework 2019–20123 Action Plan. Government of the Northwest Territories, Yellowknife, NT. p. 58. Available from https://www.enr.gov.nt.ca/sites/enr/files/resources/128-climate_change_ap_proof.pdf [accessed 2020]

GRID-Arendal. 2020. Northern issues, science gaps and recommendations. *In* Rapid response assessment of coastal and offshore permafrost, story map. Available from https://storymaps.arcgis.com/stories/74bf8d1540c542b7a444a5a2ba1559e2 [accessed April 2023].

Hjelmager, J., Moellering, H., Cooper, A., Delgado, T., Rajabifard, A., Rapant, P., et al. 2008. An initial formal model for spatial data infrastructures. International Journal of Geographical Information Science, **22**: 1295–1309. doi:10.1080/13658810801909623.

Hjort, J., Karjalainen, O., Aalto, J., Westermann, S., Romanovsky, V.E., Nelson, F.E., et al. 2018. Degrading permafrost puts Arctic infrastructure at risk by mid-century. Nature Communications, **9**. doi:10.1038/s41467-018-07557-4.

Huang, L., Luo, J., Lin, Z., Niu, F., and Liu, L. 2020. Using deep learning to map retrogressive thaw slumps in the Beiluhe region (Tibetan Plateau) from CubeSat images. Remote Sensing of Environment, **237**: 111534. doi:10.1016/j.rse.2019.111534.

Inuit Tapiriit Kanatami. 2018. National Inuit strategy on research. Available from https://www.itk.ca/wp-content/uploads/2018/04/ITK_NISR-Report_English_low_res.pdf [accessed April 2023].

Johnson, N., Alessa, L., Behe, C., Danielsen, F., Gearheard, S., Gofman-Wallingford, V., et al. 2015. The contributions of community-based monitoring and traditional knowledge to Arctic observing networks: reflections on the state of the field. Arctic, **68**: 28–40. doi:10.14430/arctic4447.

Jorgenson, M.T., Kanevskiy, M., Shur, Y., Moskalenko, N., Brown, D.R.N., Wickland, K., et al. 2015. Role of ground ice dynamics and ecological feedbacks in recent ice wedge degradation and stabilization. Journal of Geophysical Research: Earth Surface, **120**: 2280–2297. doi:10.1002/2015JF003602.

Karjalainen, O., Luoto, M., Aalto, J., Etzelmüller, B., Grosse, G., Jones, B.M., et al. 2020. High potential for loss of permafrost landforms in a changing climate. Environmental Research Letters, **15**. doi:10.1088/1748-9326/abafd5.

Keating, G.N., Rich, P.M., and Witkowski, M.S. 2003. Challenges for enterprise GIS. URISA Journal, **15**: 28.

Kerr, D.E., Plouffe, A., Campbell, J.E., and McMartin, I. 2022. Status of surficial geology mapping in the North. Geological Survey of Canada, Preprint **1**. doi:10.4095/330334.

Kokelj, S.V., and Burn, C.R. 2003. Ground ice and soluble cations in near-surface permafrost, Inuvik, Northwest Territories, Canada. Permafrost and Periglacial Processes, **14**: 275–289. doi:10.1002/ppp.458.

Kokelj, S.V., and Burn, C.R. 2004. Tilt of spruce trees near ice wedges, Mackenzie Delta, northwest territories, Canada. Arctic, Antarc-

tic, and Alpine Research, **36**: 615–623. doi:10.1657/1523-0430(2004)036[0615:TOSTNI]2.0.CO;2.

Kokelj, S.V., and Burn, C.R. 2005. Near-surface ground ice in sediments of the Mackenzie Delta, Northwest Territories, Canada. Permafrost and Periglacial Processes, **16**: 291–303. doi:10.1002/ppp.537.

Kokelj, S.V., and Jorgenson, M.T. 2013. Advances in thermokarst research. Permafrost and Periglacial Processes, **24**: 108–119. doi:10.1002/ppp.1779.

Kokelj, S.V., Lantz, T.C., Wolfe, S.A., Kanigan, J.C., Morse, P.D., Coutts, R., et al. 2014. Distribution and activity of ice wedges across the forest-tundra transition, western arctic Canada. Journal of Geophysical Research: Earth Surface, **119**: 2032–2047. doi:10.1002/2014JF003085.

Kokelj, S.V., Tunnicliffe, J., Lacelle, D., Lantz, T.C., Chin, K.S., and Fraser, R. 2015. Increased precipitation drives mega slump development and destabilization of ice-rich permafrost terrain, northwestern Canada. Global and Planetary Change, **129**: 56–68. doi:10.1016/j.gloplacha.2015.02.008.

Kokelj, S.V., Lantz, T.C., Tunnicliffe, J., Segal, R., and Lacelle, D. 2017. Climate-driven thaw of permafrost preserved glacial landscapes, northwestern Canada. Geology, **45**: 371–374. doi:10.1130/G38626.1.

Kokelj, S.V., Kokoszka, J., van der Sluijs, J., Rudy, A.C.A., Tunnicliffe, J., Shakil, S., et al. 2021. Thaw-driven mass wasting couples slopes with downstream systems, and effects propagate through Arctic drainage networks. The Cryosphere, **15**: 3059–3081. doi:10.5194/tc-15-3059-2021.

Kong, N.N. 2015. Exploring best management practices for geospatial data in academic libraries. Journal of Map & Geography Libraries, **11**: 207–225. doi:10.1080/15420353.2015.1043170.

Lantz, T.C., Kokelj, S.V., Gergel, S.E., and Henry, G.H.R. 2009. Relative impacts of disturbance and temperature: persistent changes in microenvironment and vegetation in retrogressive thaw slumps. Global Change Biology, **15**: 1664–1675. doi:10.1111/j.1365-2486.2009.01917.x.

Lantz, T., Steedman, A., Kokelj, S.V., and Segal, R. 2017. Inventory of polygonal terrain in the Tuktoyaktuk Coastlands, Northwest Territories. NWT Open Report 2016–22. Northwest Territories Geological Survey, Yellowknife, NT. p. 10. doi:10.46887/2016-022.

Lantz, T.C., Zhang, Y., and Kokelj, S.V. 2022. Impacts of ecological succession and climate warming on permafrost aggradation in drained lake basins of the Tuktoyaktuk Coastlands, Northwest Territories, Canada. Permafrost & Periglacial Processes, **33**: 176–192. doi:10.1002/ppp.2143.

Lewkowicz, A.G., and Way, R.G. 2019. Extremes of summer climate trigger thousands of thermokarst landslides in a High Arctic environment. Nature Communications, **10**. doi:10.1038/s41467-019-09314-7.

MacEachren, A.M. 2001. Cartography and GIS: extending collaborative tools to support virtual teams. Progress in Human Geography, **25**: 431–444. doi:10.1191/030913201680191763.

Mackay, J.R. 1972. The world Of underground ice. Annals of the Association of American Geographers, **62**: 1–22. doi:10.1111/j.1467-8306.1972.tb00839.x.

Maguire, D.J., and Longley, P.A. 2005. The emergence of geoportals and their role in spatial data infrastructures. Computers, Environment and Urban Systems, **29**: 3–14. doi:10.1016/j.compenvurbsys.2004.05.012.

Maquil, V., Leopold, U., de Sousa, L.M., Schwartz, L., and Tobias, E. 2018. Towards a framework for geospatial tangible user interfaces in collaborative urban planning. Journal of Geographical Systems, **20**: 185–206. doi:10.1007/s10109-018-0265-6.

Marsh, P., Russell, M., Pohl, S., Haywood, H., and Onclin, C. 2009. Changes in thaw lake drainage in the Western Canadian Arctic from 1950 to 2000. Hydrological Processes, **23**: 145–158. doi:10.1002/hyp.7179.

Michener, W.K. 2015. Ecological data sharing. Ecological Informatics, **29**: 33–44. doi:10.1016/j.ecoinf.2015.06.010.

Morse, P.D., and Rudy, A.C.A. 2022. Distributions of degraded and intact lithalsas, North Slave region, Northwest Territories. *In* Geological Survey of Canada, open file 8869. doi:10.4095/329643.

Morse, P.D., McWade, T.L., and Wolfe, S.A. 2017. Thermokarst ponding, North Slave region, Northwest Territories. *In* Geological Survey of Canada, open file 8205. doi:10.4095/300531.

Murton, J.B., Whiteman, C.A., Waller, R.I., Pollard, W.H., Clark, I.D., and Dallimore, S.R. 2005. Basal ice facies and supraglacial melt-out till of the Laurentide Ice Sheet, Tuktoyaktuk Coastlands, western Arc-

tic Canada. Quaternary Science Reviews, **24**: 681–708. doi:10.1016/j.quascirev.2004.06.008.

National Geological Surveys Committee. 2022. Intergovernmental Geoscience Accord. Catalogue number: M34-74/2022E-PDF. p. 9. Available from https://www.geologicalsurveys.ca/sites/ngsc-admin/files/2022-08/intergovernmental-geoscience-accord-2022-bilingual.pdf [accessed April 2023].

Natural Resources Canada. 2015. Canada digital elevation data [dataset]. Natural Resources Canada, Ottawa, ON. Available from https://open.canada.ca/data/en/dataset/7f245e4d-76c2-4caa-951a-45d1d2051333 [accessed 2020].

Natural Resources Canada. 2016. National Hydro Network – NHN – GeoBase Series [dataset]. Canadian Council on Geomatics Geobase, Ottawa, ON. Available from https://open.canada.ca/data/en/dataset/a4b190fe-e090-4e6d-881e-b87956c07977 [accessed 2021].

Nitze, I., Grosse, G., Jones, B.M., Romanovsky, V.E., and Boike, J. 2018. Remote sensing quantifies widespread abundance of permafrost region disturbances across the Arctic and Subarctic. Nature Communications, **9**. doi:10.1038/s41467-018-07663-3.

Olefeldt, D., Goswami, S., Grosse, G., Hayes, D., Hugelius, G., Kuhry, P., et al. 2016. Circumpolar distribution and carbon storage of thermokarst landscapes. Nature Communications, **7**. doi:10.1038/ncomms13043.

O'Neill, H.B., and Burn, C.R. 2012. Physical and temporal factors controlling the development of near-surface ground ice at Illisarvik, Western Arctic coast, Canada. Canadian Journal of Earth Sciences, **49**: 1096–1110. doi:10.1139/E2012-043.

O'Neill, H.B., Wolfe, S.A., and Duchesne, C. 2019. New ground ice maps for Canada using a paleogeographic modelling approach. The Cryosphere, **13**: 753–773. doi:10.5194/tc-13-753-2019.

O'Neill, H.B., Wolfe, S.A., and Duchesne, C. 2022. Ground ice map of Canada (2022) [dataset] Natural Resources Canada GEOSCAN. doi:10.4095/330294.

Pasher, J., Seed, E., and Duff, J. 2013. Development of boreal ecosystem anthropogenic disturbance layers for Canada based on 2008 to 2010 Landsat imagery. Canadian Journal of Remote Sensing, **39**: 42–58. doi:10.5589/m13-007.

Paul, J.R., Kokelj, S.V., and Baltzer, J.L. 2021. Spatial and stratigraphic variation of near-surface ground ice in discontinuous permafrost of the Taiga Shield. Permafrost and Periglac Processes, **32**: 3–18. doi:10.1002/ppp.2085.

Pulsifer, P.L., Laidler, G.J., Taylor, D.R.F., and Hayes, A. 2011. Towards an Indigenist data management program: reflections on experiences developing an atlas of sea ice knowledge and use. Canadian Geographer, **55**: 108–124. doi:10.1111/j.1541-0064.2010.00348.x.

Quinton, W.L., Hayashi, M., and Chasmer, L.E. 2011. Permafrost-thaw-induced land-cover change in the Canadian subarctic: implications for water resources. Hydrological Processes, **25**: 152–158. doi:10.1002/hyp.7894.

Rampton, V.N. 1988. Quaternary geology of the Tuktoyaktuk Coastlands, Northwest Territories. *In* Geological Survey of Canada, Memoir 423. doi:10.4095/126937.

Ramsdale, J.D., Balme, M.R., Conway, S.J., Gallagher, C., van Gasselt, S.A., Hauber, E., et al. 2017. Grid-based mapping: a method for rapidly determining the spatial distributions of small features over very large areas. Planetary and Space Science, **140**: 49–61. doi:10.1016/j.pss.2017.04.002.

Schuur, E.A.G., and Mack, M.C. 2018. Ecological response to permafrost thaw and consequences for local and global ecosystem services. Annual Review of Ecology, Evolution, and Systematics, **49**: doi:10.1146/annurev-ecolsys-121415-032349.279.

Segal, R.A., Kokelj, S.V., Lantz, T.C. Pierce, K.L. Durkee, K. Gervais, S. Mahon, E. Snijders, M. Buysse, J. and Schwarz, S. 2016. Mapping of terrain affected by retrogressive thaw slumping in northwestern Canada. NWT Open Report 2016-023. Northwest Territories Geological Survey, Yellowknife, NT. p. 5. doi:10.46887/2016-023.

Siewert, M.B. 2018. High-resolution digital mapping of soil organic carbon in permafrost terrain using machine learning: a case study in a sub-Arctic peatland environment. Biogeosciences, **15**: 1663–1682. doi:10.5194/bg-15-1663-2018.

Sladen, W.E., Parker, R.J.H., Morse, P.D., Kokelj, S.V., and Smith, S.L. 2022. Geomorphic feature inventory along the Dempster and Inuvik to Tuk-

toyaktuk highway corridor, Yukon and Northwest Territories. *In* Geological Survey of Canada, open file 8885. doi:10.4095/329969.

Slaymaker, O., and Kovanen, D.J. 2017. Pleistocene landscapes of western Canada. *In* Landscapes and landforms of western Canada. World geomorphic landscapes. *Edited by* O. Slaymaker. Springer, Cham, Switzerland. doi:10.1007/978-3-319-44595-3_2.

Smith, S.L., Romanovsky, V.E., Lewkowicz, A.G., Burn, C.R., Allard, M., Clow, G.D., et al. 2010. Thermal state of permafrost in North America: a contribution to the international polar year. Permafrost and Periglacial Processes, **21**: 117–135. doi:10.1002/ppp.690.

Smith, S.L., O'Neill, H.B., Isaksen, K., Noetzli, J., and Romanovsky, V.E. 2022. The changing thermal state of permafrost. Nature Reviews Earth and Environment, 3: 10–23. doi:10.1038/s43017-021-00240-1.

Spence, C., Norris, M., Bickerton, G., Bonsal, B.R., Brua, R., Culp, J.M., et al. 2020. The Canadian water resource vulnerability index to permafrost thaw (Cwrvipt). Arctic Science, **6**. doi:10.1139/as-2019-0028.

Spring, A., Carter, B., and Blay-Palmer, A. 2018. Climate change, community capitals, and food security: building a more sustainable food system in a northern Canadian boreal community. Canadian Food Studies / La Revue canadienne des études sur l'alimentation, 5: 111–141. doi:10.15353/cfs-rcea.v5i2.199.

Steedman, A.E., Lantz, T.C., and Kokelj, S.V. 2017. Spatio-temporal variation in high-centre polygons and ice-wedge melt ponds, Tuktoyaktuk Coastlands, Northwest Territories. Permafrost and Periglacial Processes, **28**: 66–78. doi:10.1002/ppp.1880.

Tank, S.E., Vonk, J.E., Walvoord, M.A., McClelland, J.W., Laurion, I., and Abbott, B.W. 2020. Landscape matters: predicting the biogeochemical effects of permafrost thaw on aquatic networks with a state factor approach. Permafrost and Periglacial Processes, **31**: 358–370. doi:10.1002/ppp.2057.

Thompson, K.-L., Lantz, T., and Ban, N. C. 2020. A review of Indigenous knowledge and participation in environmental monitoring. Ecology and Society, **25**(2): 10. doi:10.5751/ES-11503-250210.

Tobler, W. 1987. Measuring spatial resolution. Proposed to the Beijing Conference on Land Use and Remote Sensing. Available from https://www.researchgate.net/publication/291877360_Measuring_spatial_resolution [accessed 2022].

Turetsky, M.R., Abbott, B.W., Jones, M.C., Anthony, K.W., Olefeldt, D., Schuur, E.A.G., et al. 2020. Carbon release through abrupt permafrost thaw. Nature Geoscience, **13**: 138–143. doi:10.1038/s41561-019-0526-0.

Turner, K.W., Pearce, M.D., and Hughes, D.D. 2021. Detailed characterization and monitoring of a retrogressive thaw slump from remotely piloted aircraft systems and identifying associated influence on carbon and nitrogen export. Remote Sensing, **13**: 171. doi:10.3390/rs13020171.

van der Sluijs, J., Kokelj, S. v., Fraser, R.H., Tunnicliffe, J., and Lacelle, D. 2018. Permafrost terrain dynamics and infrastructure impacts revealed by UAV photogrammetry and thermal imaging. Remote Sensing, **10**. doi:10.3390/rs10111734.

van der Sluijs, J., Kokelj, S.V., and Tunnicliffe, J.F. 2022. Allometric scaling of retrogressive thaw slumps. The Cryosphere Discussions, **2022**: 1–30. doi:10.5194/tc-2022-149.

Vitt, D.H., Halsey, L.A., and Zoltai, S.C. 1994. The bog landforms of continental western Canada in relation to climate and permafrost patterns. Arctic and Alpine Research, **26**: 1–13. doi:10.2307/1551870.

Wang, S. 2010. A CyberGIS framework for the synthesis of cyberinfrastructure, GIS, and spatial analysis. Annals of the Association of American Geographers, **100**: 535–557. doi:10.1080/00045601003791243.

Wang, Y., Way, R.G., Beer, J., Forget, A., Tutton, R., and Purcell, M.C. 2023. Significant underestimation of peatland permafrost along the Labrador Sea coastline in northern Canada. The Cryosphere, **17**: 63–78. doi:10.5194/tc-17-63-2023.

Wolfe, S.A., and Morse, P.D. 2017. Lithalsa formation and Holocene lake-level recession, Great Slave Lowland, Northwest Territories. Permafrost and Periglacial Processes, **28**: 573–579. doi:10.1002/ppp.1901.

Wolfe, S.A., Short, N.H., Morse, P.D., Schwarz, S.H., and Stevens, C.W. 2014. Evaluation of RADARSAT-2 DInSAR seasonal surface displacement in discontinuous permafrost terrain, Yellowknife, Northwest Territories, Canada. Canadian Journal of Remote Sensing, **40**: 406–422. doi:10.1080/07038992.2014.1012836.

Wolfe, S., Kokelj, S.V., Paul, J., and Gingras-Hill, T. 2022. Northwest Territories Thermokarst Mapping Collective: procedural manual for sentinel image classification of hydrological features in permafrost terrain. NWT Open Report. Northwest Territories Geological Survey, Yellowknife, NT. p. 46. doi:10.46887/2021-007.

Wolfe, S.A., Morse, P.D., Parker, R., and Phillips, M.R. 2023. Distribution and morphometry of pingos, western Canadian Arctic, Northwest Territories, Canada. Geomorphology, **431**: 108694. doi:10.1016/j.geomorph.2023.108694.

Young, J. M., Alvarez, A., van der Sluijs, J., Kokelj, S. V., Rudy, A., McPhee, A., et al. 2022. Recent intensification (2004–2020) of permafrost mass-wasting in the central Mackenzie Valley foothills is a legacy of past forest fire disturbances. Geophysical Research Letters, **49**. doi:10.1029/2022GL100559.

Yovcheva, Z., van Elzakker, C.P.J.M., and Köbben, B. 2013. User requirements for geo-collaborative work with spatio-temporal data in a web-based virtual globe environment. Applied Ergonomics, **44**: 929–939. doi:10.1016/j.apergo.2012.10.015.

Zwieback, S., Kokelj, S.V., Gunther, F., Boike, J., Grosse, G., and Hajnsek, I. 2018. Sub-seasonal thaw slump mass wasting is not consistently energy limited at the landscape scale. The Cryosphere, **12**: 549–564. doi:10.5194/tc-12-549-2018.

Appendix A

Examples of features mapped in Figs. 7–9. (A) Oblique photos are from summers of 2020–2022 and can be accessed at: https://www.apps.geomatics.gov.nt.ca/arcgis/rest/services/GNWT_Operational/NTGS_ThermokarstCollective_Operational/MapServer, (B) circa 2018 SPOT 6/7 true color imagery at 1.5 m resolution (© 2018 Airbus Defence and Space, licensed by Planet Labs Geomatics Corp.), and (C) 2016–2017 Sentinel-2 peak-summer false colour imagery at 10 m spatial resolution (European Space Agency, Copernicus Sentinel data).

Plate. 1. (A) Oblique aerial photograph of a lakeside retrogressive thaw slump (RTS) in ice-rich glaciated terrain of the Caribou Hills (133.6828167°W, 68.7797350°N); (B) SPOT 6/7 imagery (© 2018 Airbus Defence and Space, licensed by Planet Labs Geomatics Corp.); and (C) Sentinel-2 imagery (European Space Agency, Copernicus Sentinel data) showing the active, lakeside RTS indicated by the arrow. Note the debris tongue extending into the adjacent lake, and that the lower parts of the thaw slump were vegetated by August 2021 when the photograph was taken.
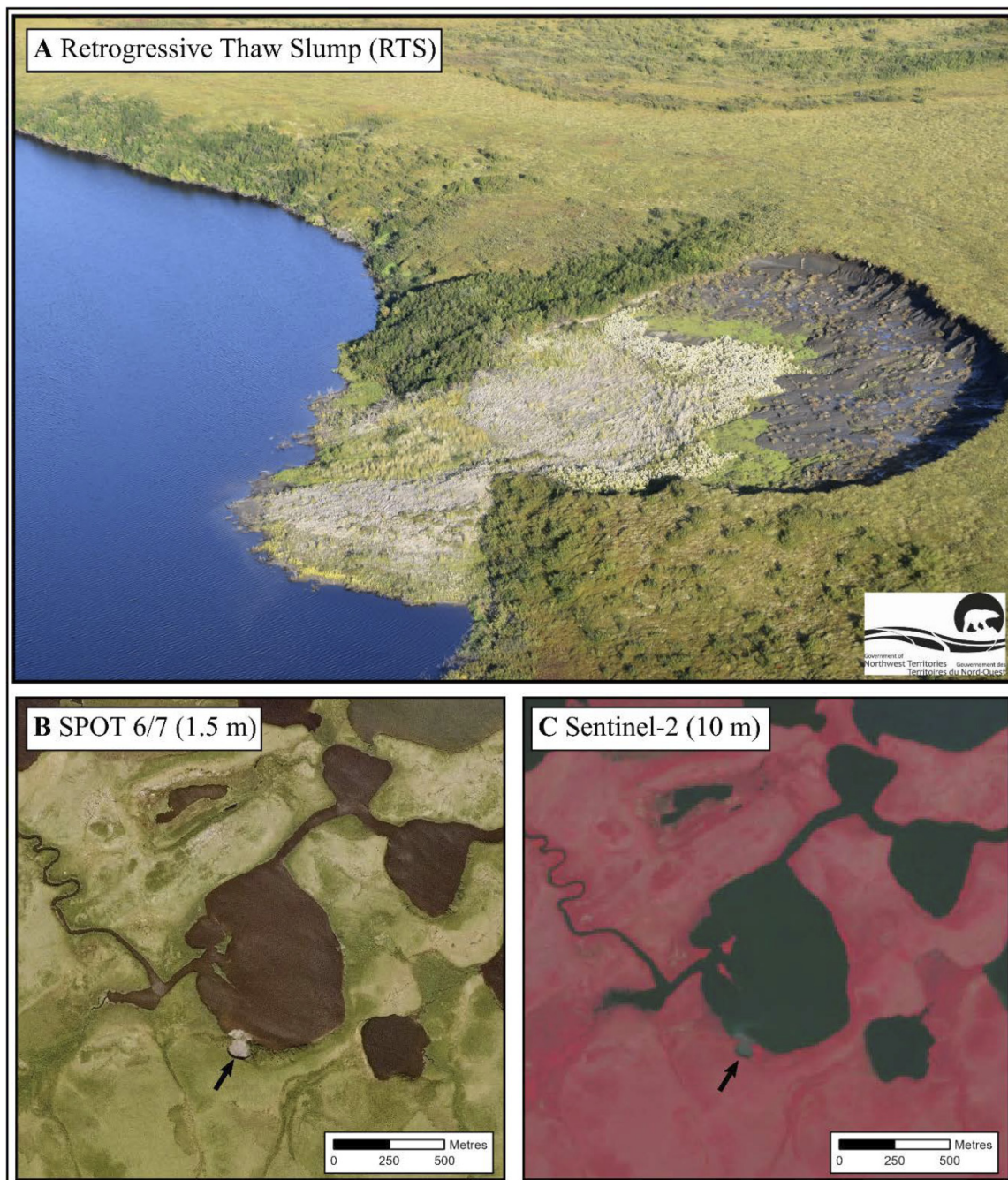
Plate. 2. (A) Oblique aerial photograph of a RTS with a well-developed active headwall and debris tongue deposit located in ice-rich glaciated terrain of the Richardson Mountains (135.58958°W, 67.96898°N); (B) the RTS in the photograph is indicated with a large black arrow on the SPOT 6/7 imagery (© 2018 Airbus Defence and Space, licensed by Planet Labs Geomatics Corp.); and on the (C) Sentinel-2 near-infrared imagery (European Space Agency, Copernicus Sentinel data). A small hollow arrow indicates another RTS on the upper right of the imagery, and a thin arrow shows a prominent cuspate-shaped colluvial slope cut into the bedrock by stream erosion.
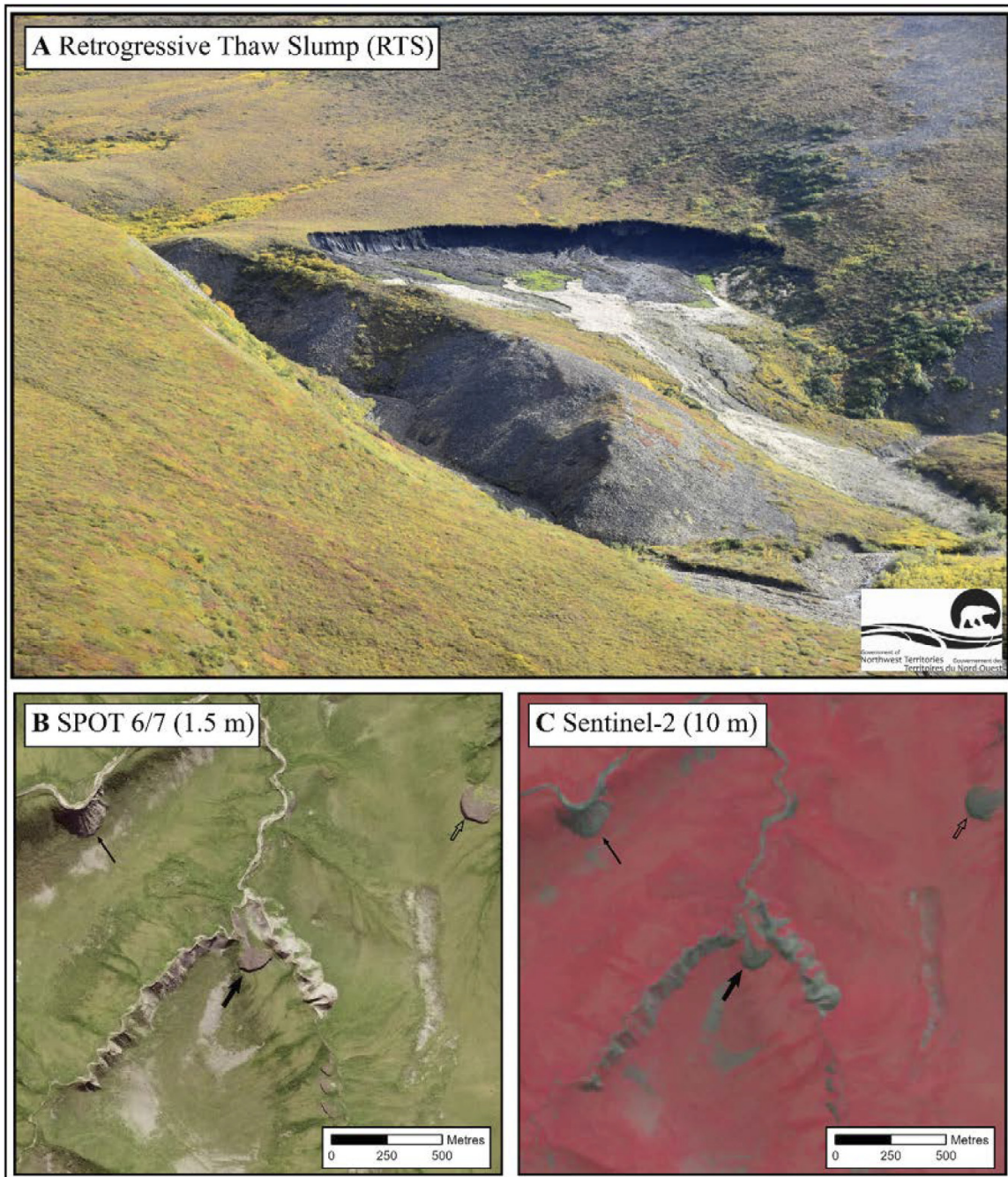
Plate. 3. (A) Oblique aerial photograph of a RTS and large debris tongue deposit from the Mackenzie Foothills (125.9701330°W, 64.0443845°N); (B) the large RTS in the photograph is indicated with a filled arrow on the SPOT 6/7 imagery (© 2018 Airbus Defence and Space, licensed by Planet Labs Geomatics Corp.); and on the (C) Sentinel-2 imagery (European Space Agency, Copernicus Sentinel data). The hollow arrow indicates a small RTS which is visible on (B) and (C). Bare bedrock outcrops and unvegetated colluvial slopes are visible on the left-hand side of the image plates.
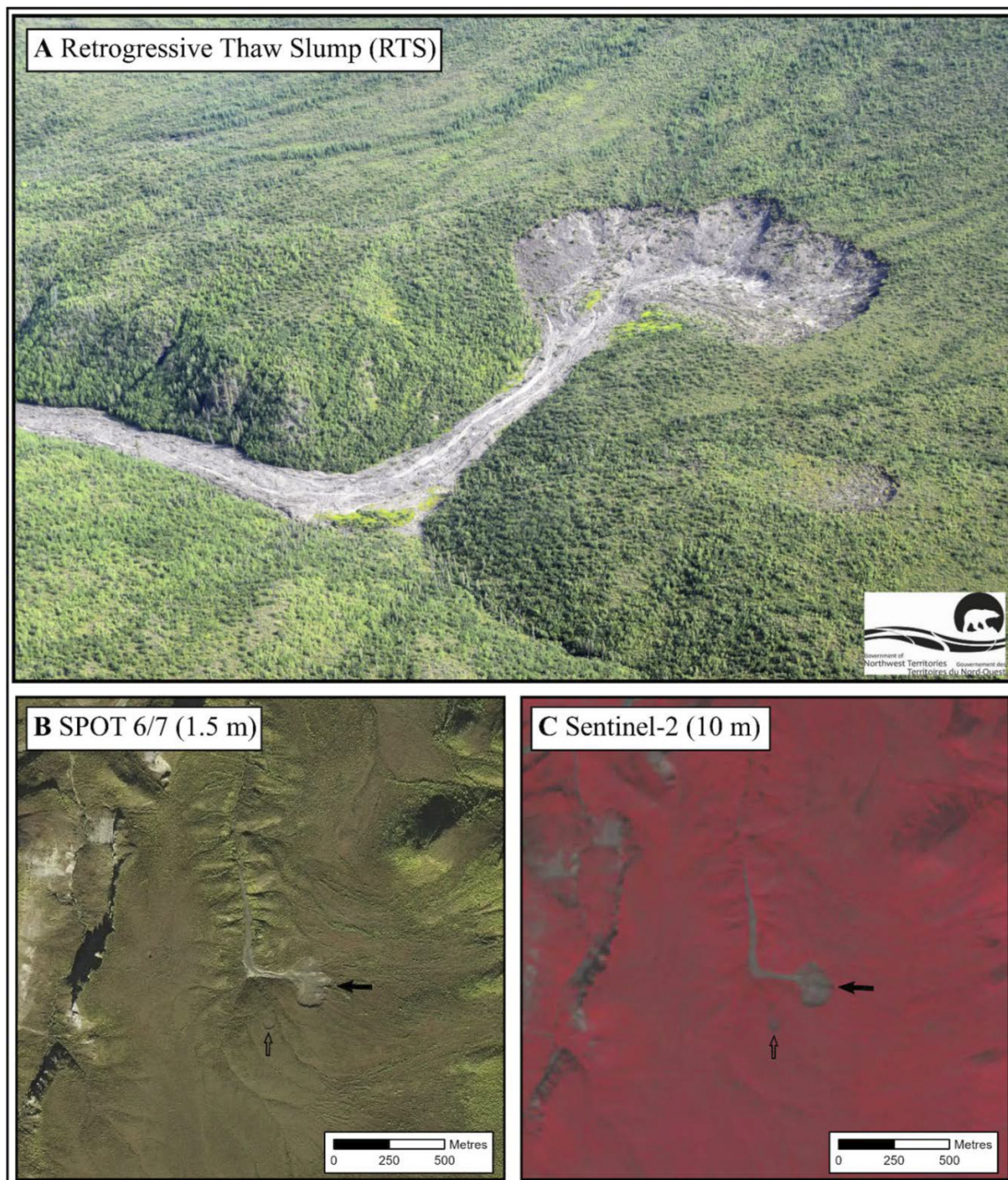
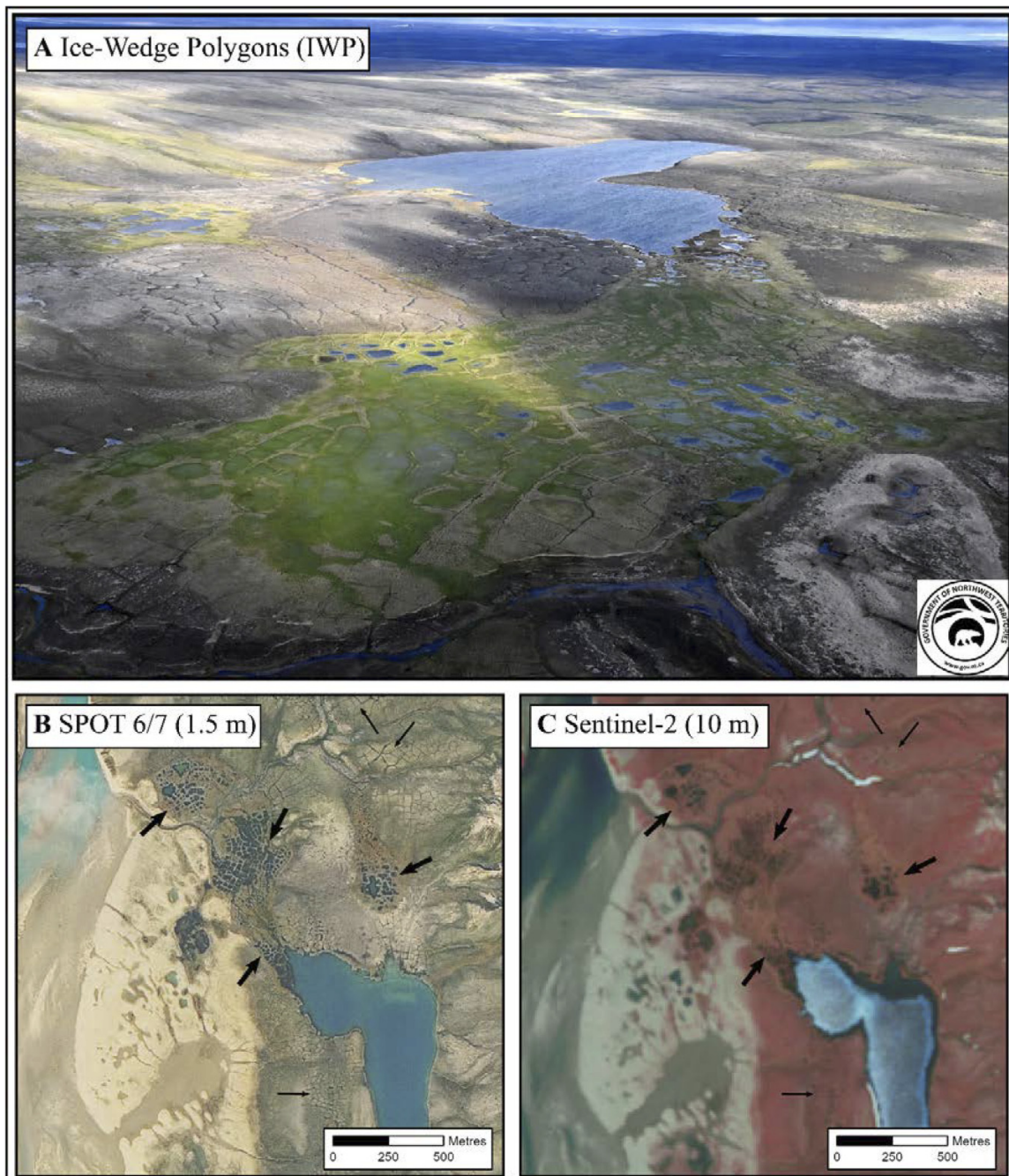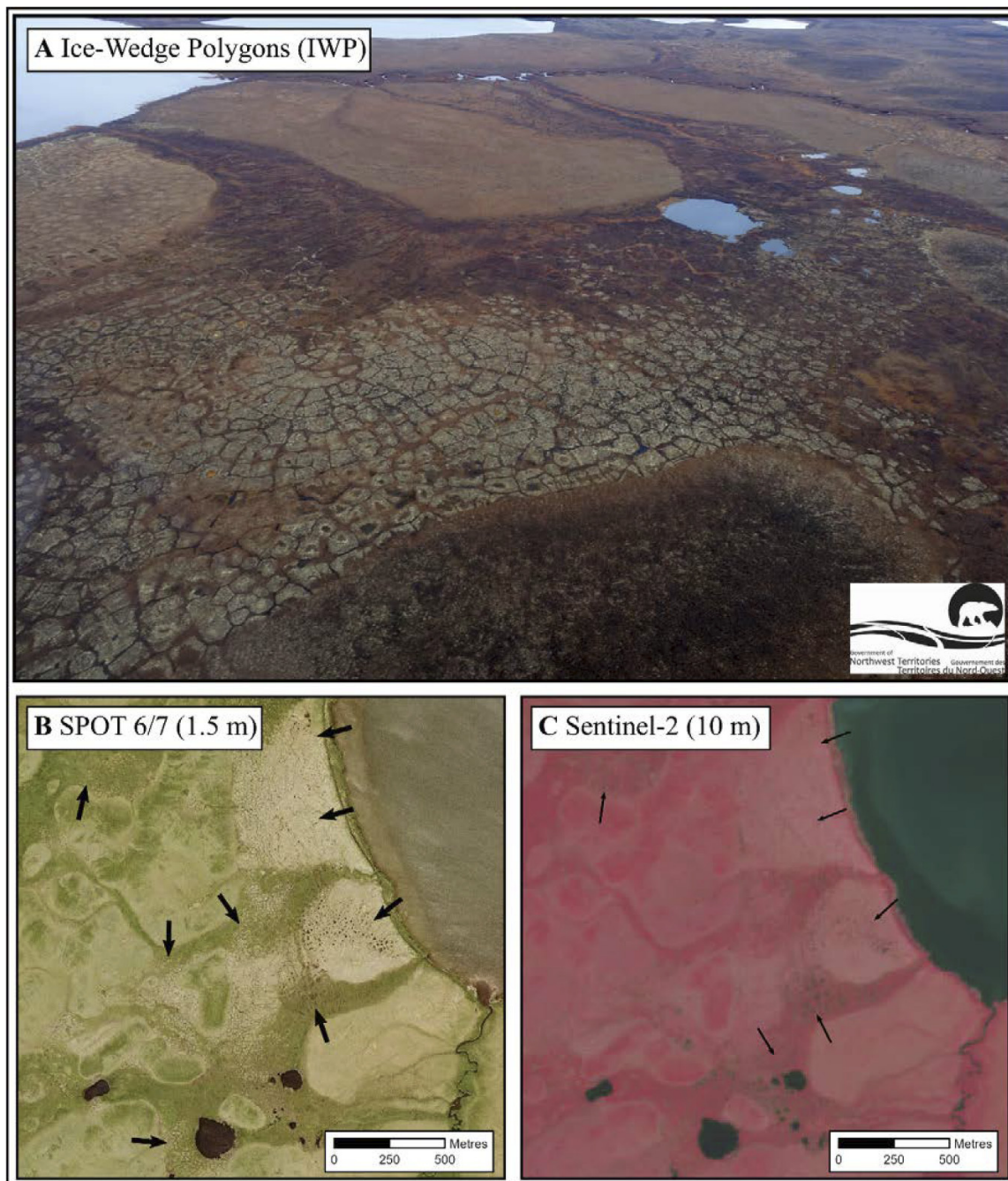**Plate. 4.** (A) Oblique aerial photograph of low- and high-centred polygons in lowland terrain, and high-centred polygons on adjacent hills (upland terrain) of the Thomsen Valley (119.8903964°W, 73.7705192°N), Banks Island; (B) SPOT 6/7 (© 2018 Airbus Defence and Space, licensed by Planet Labs Geomatics Corp.); and (C) Sentinel-2 imagery (European Space Agency, Copernicus Sentinel data) showing well-defined polygonal-patterned ponding in low- and high-centred polygons of low-lying areas (larger black arrows), and high-centred polygons in adjacent hilly uplands (small arrows).

Plate. 5. (A) Oblique aerial photograph of low- and high-centred polygonal peatlands in lowland terrain and high-centred polygons in adjacent, more elevated terrain of the Caribou Hills (133.8021694°W 68.8445256°N) north of Inuvik; (B) SPOT 6/7 imagery (© 2018 Airbus Defence and Space, licensed by Planet Labs Geomatics Corp.) showing patterns of high- and low-centred polygons in low-lying areas and in the adjacent hilly terrain indicated by black arrows; and (C) Sentinel-2 imagery (European Space Agency, Copernicus Sentinel data) showing textured areas indicative of polygonal terrain indicated by small arrows.

Plate. 6. (A) Oblique aerial photograph of a discrete high-centred polygonal peatland on the Sitidgi Plain (133.3891629°W, 68.3615730°N); (B) SPOT 6/7 imagery (© 2018 Airbus Defence and Space, licensed by Planet Labs Geomatics Corp.) with arrows showing the polygonal peatlands; and (C) Sentinel-2 imagery (European Space Agency, Copernicus Sentinel data) with thin arrows showing patterns of polygonal peatlands and rectangular drainage.
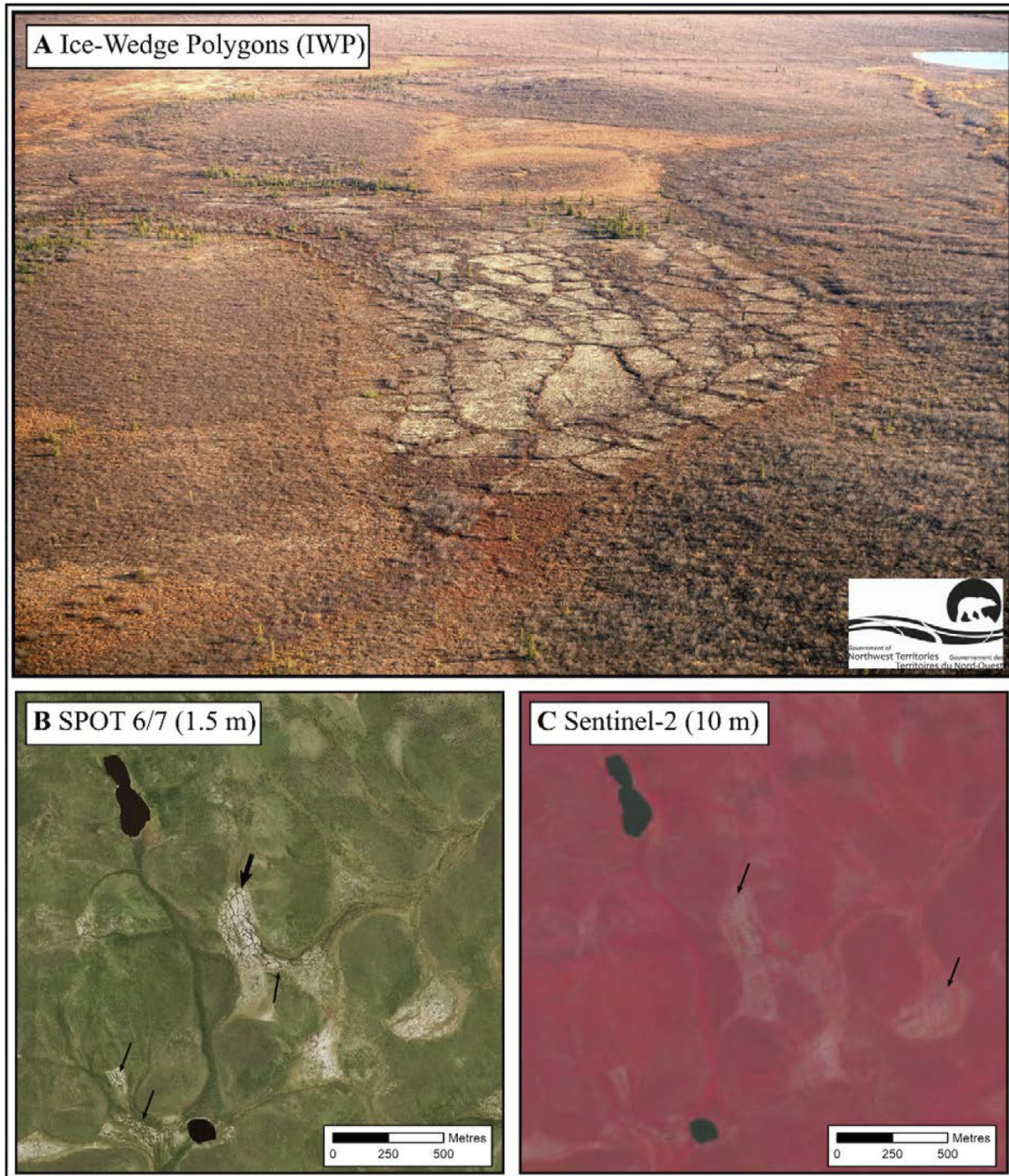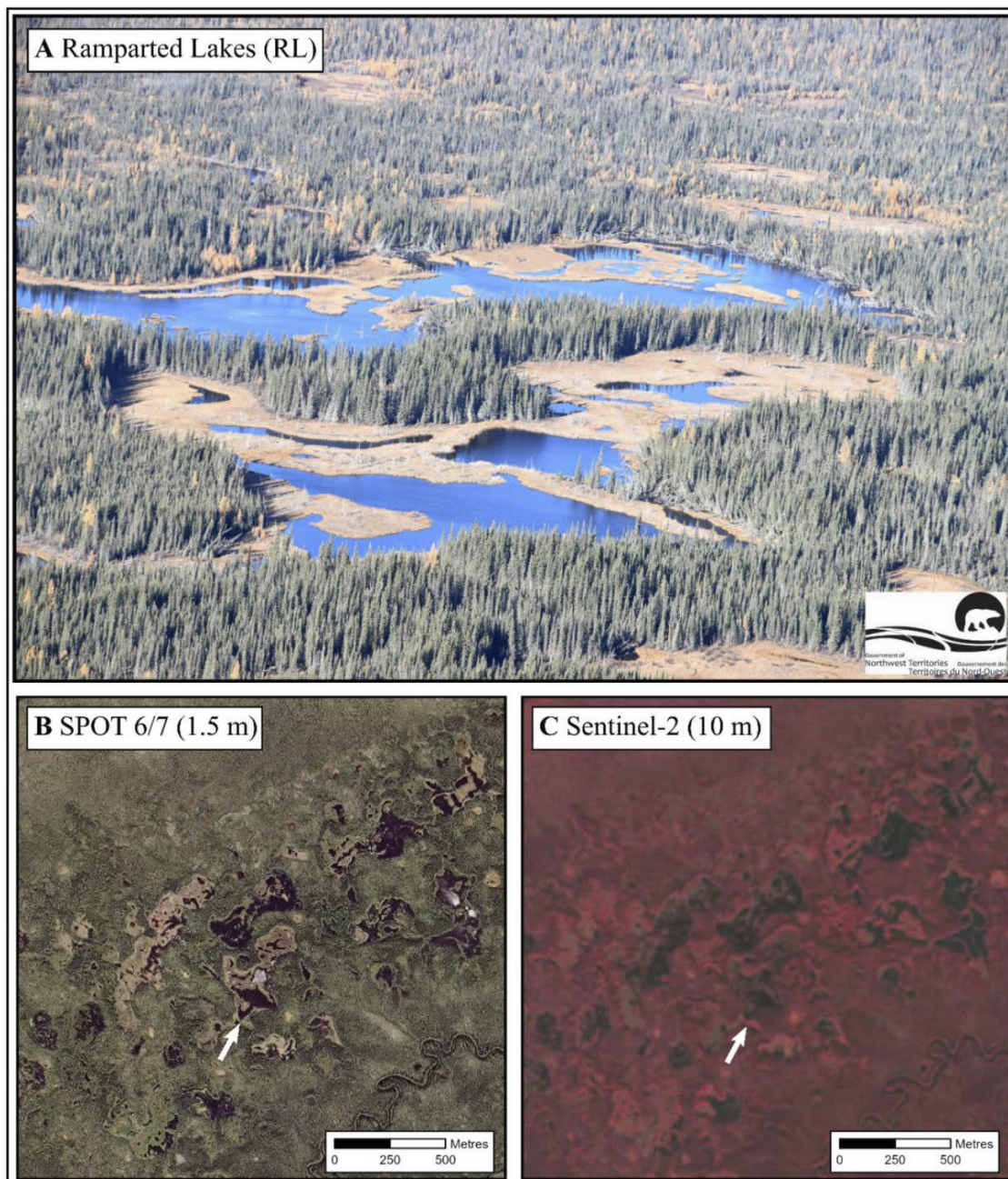
Plate. 7. (A) Oblique aerial photograph of a large contiguous area of ramparted lake–lithalsa (RL–L) complexes (thermokarst lake complexes) with "undifferentiated (thermokarst) patterned ponding" in ice-rich glaciolacustrine deposits on the Great Slave Plain–High Boreal area (116.59785°W, 62.99697°N); (B) SPOT 6/7 imagery (© 2018 Airbus Defence and Space, licensed by Planet Labs Geomatics Corp.) shows the RL–L complexes characterized by irregularly shaped lakes, undifferentiated patterned ponding, and evidence of lowered water levels; and (C) Sentinel-2 imagery (European Space Agency, Copernicus Sentinel data) shows the same landforms with textural differences reflecting lowered water levels, as well as mixed forests typically found on elevated, well-drained lithalsas. The white arrow indicates the direction from which the oblique photograph was taken.

Plate. 8. (A) Oblique aerial photograph of a localized RL–L complex in ice-rich glaciolacustrine deposits on the Great Slave Lowland–High Boreal (115.23839°W, 62.65948°N), with "undifferentiated (thermokarst) patterned ponding", and collapsing shoreline and drowned forest in the foreground and surrounded by Precambrian bedrock; (B) SPOT 6/7 imagery (© 2018 Airbus Defence and Space, licensed by Planet Labs Geomatics Corp.); and (C) the Sentinel-2 (European Space Agency, Copernicus Sentinel data) imagery shows the RL–L complex, and the arrow indicates the direction from which the oblique photograph (A) was taken.
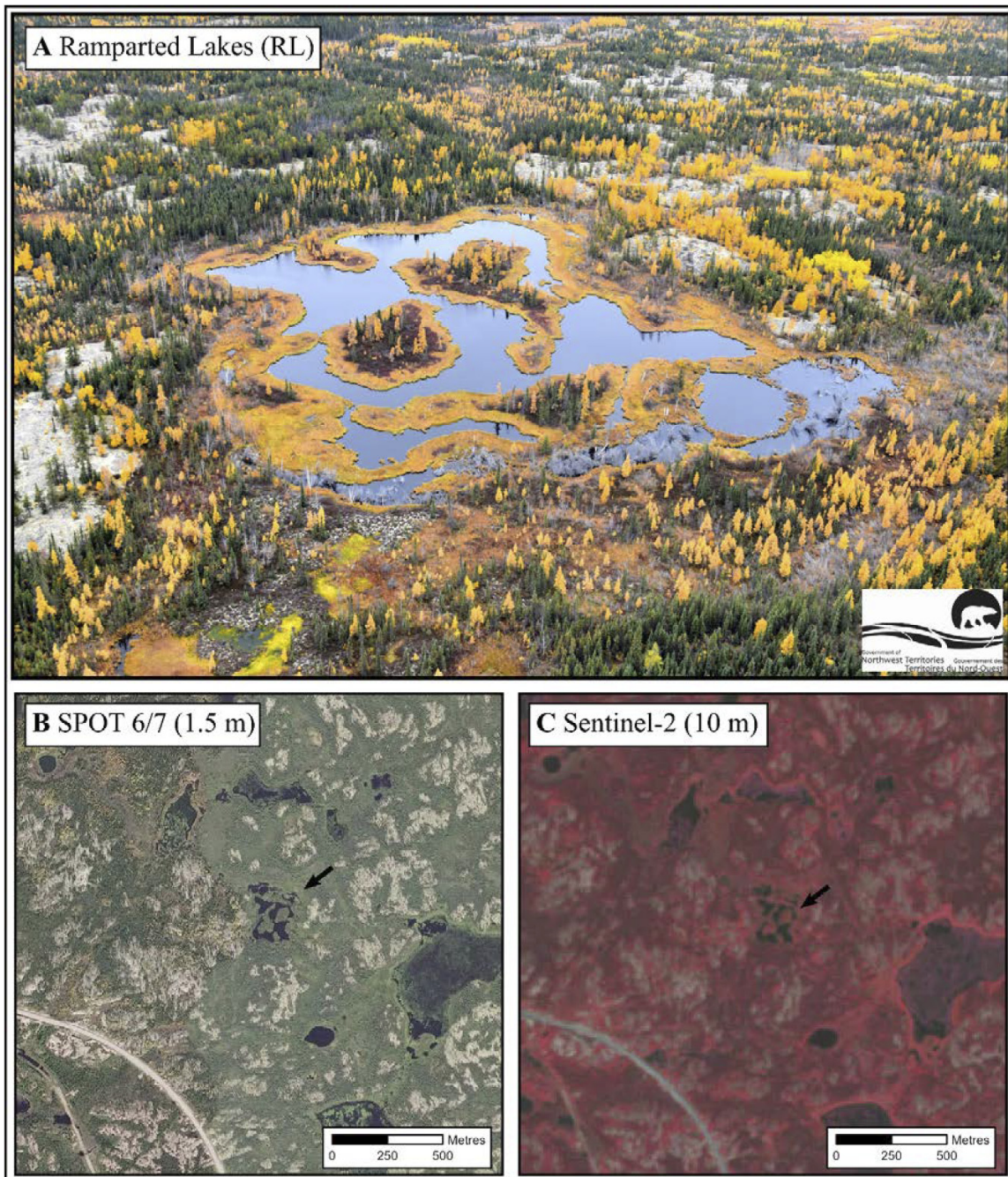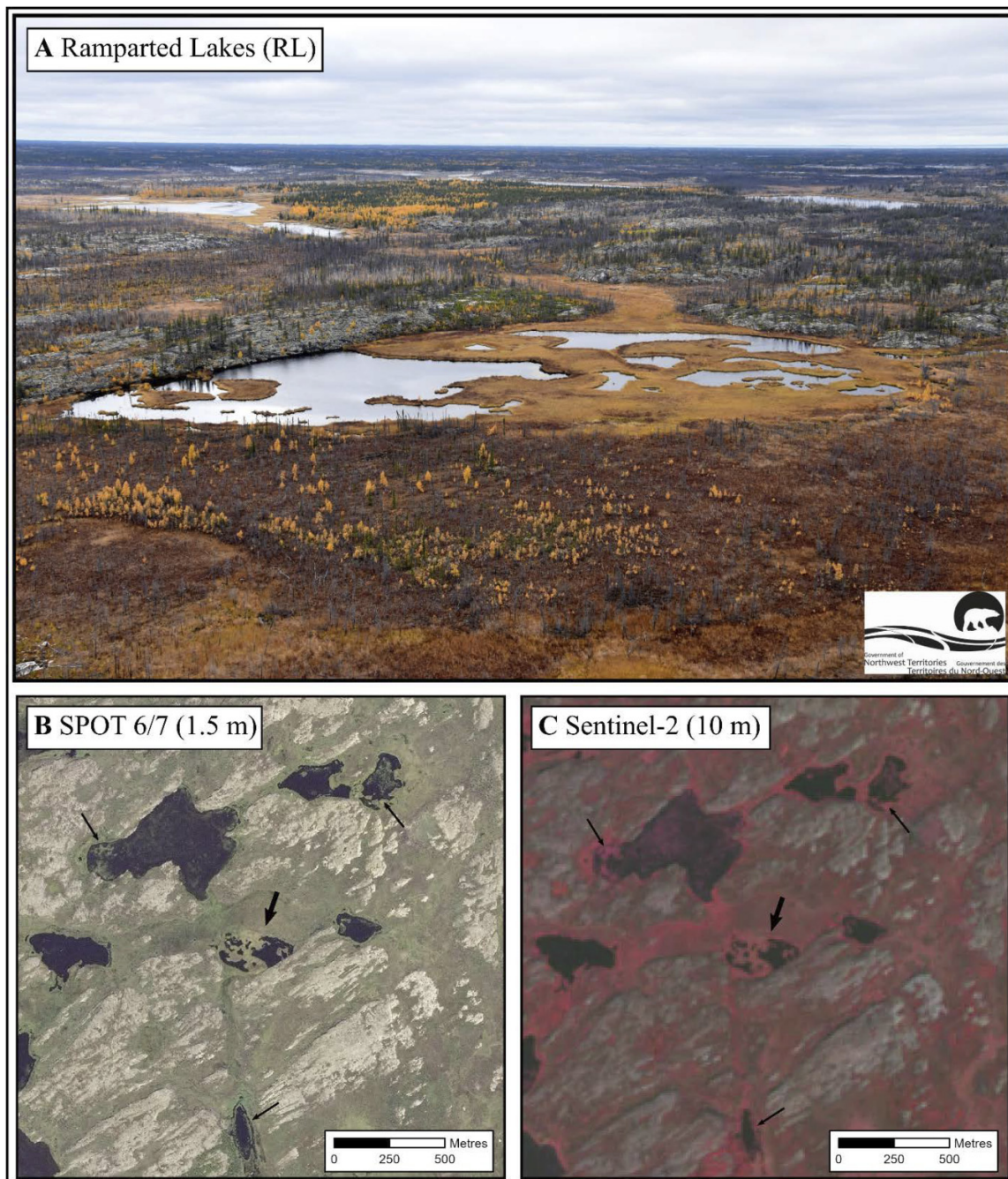
Plate. 9. (A) Oblique aerial photograph of a RL–L complex in ice-rich glaciolacustrine deposits on the Great Slave Lowland–High Boreal (114.8621658°W 62.6408444°N); (B) SPOT 6/7 imagery (© 2018 Airbus Defence and Space, licensed by Planet Labs Geomatics Corp.); and (C) the Sentinel-2 imagery (European Space Agency, Copernicus Sentinel data) showing the RL–L complex and surrounding bedrock with a shaded arrow indicating the direction from which the oblique photograph (A) was taken. Small arrows indicate other discrete RL–L features visible on the imagery.